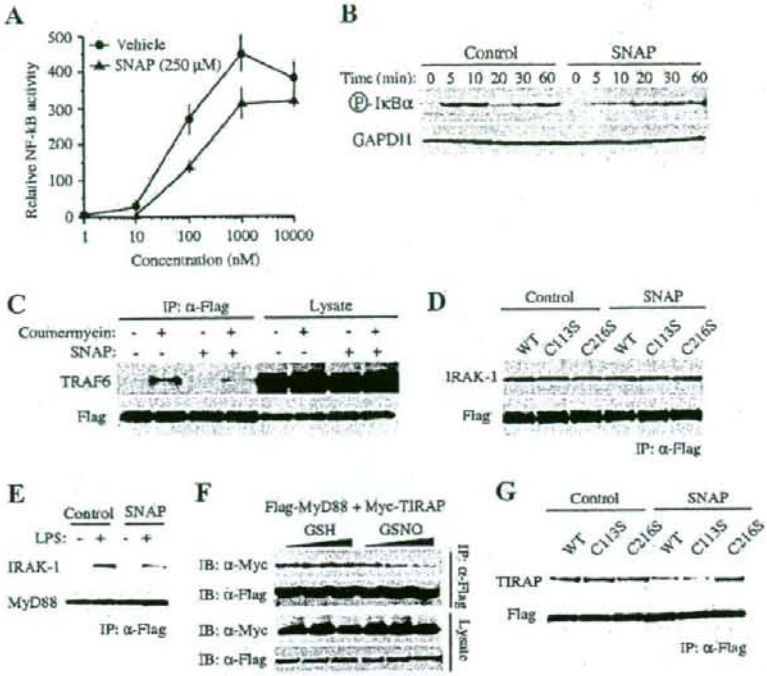

FIG. 3. Effects of NO on TLR-mediated signaling events. (A) HEK293 cells stably expressing MyD88-GyrB were transiently transfected wi an NF-κB-driven luciferase gene and incubated for 24 h. Cells were pretreated with or without 0.25 mM SNAP for 1 h and then treated with μM coumermycin for 3 h. Then, luciferase activity was measured. Each value is the mean ± SD (n = 3). (B) HEK293 cells stably expressi MyD88-GyrB were pretreated with or without 0.25 mM SNAP for 1 h and then treated with 1 μM coumermycin for the indicated periods. T phosphorylation of IκBα at Ser32/Ser36 was detected by immunoblot analysis. (C) HEK293 cells stably expressing MyD88-GyrB were pretreat with or without 0.25 mM SNAP for 1 h and then treated with 1 μM coumermycin for 20 min. Then, cell lysates were immunoprecipitated (IP) wi anti-Flag antibody, followed by immunoblotting with anti-Flag and anti-TRAF6 antibodies. (D) HEK293 cells transiently expressing Flag-tagg wild-type (WT) or Cys residue (113 or 216) replacement MyD88 together with IRAK-1 were treated with 500 μM SNAP for 1 h. Then, cell lysat were immunoprecipitated with anti-Flag antibody, followed by immunoblotting with anti-Flag and anti-IRAK-1 antibodies. (E) 293-TLR4/MD CD14 cells stably expressing Flag-MyD88-GyrB were treated with or without 500 μM SNAP for 1 h and then stimulated with 100 ng/ml LPS f 20 min. Then, cell lysates were immunoprecipitated with anti-Flag antibody, followed by immunoblotting with anti-IRAK-1 and anti-Fl antibodies. (F) HEK293 cells transiently expressing Flag-tagged MyD88 together with Myc-tagged TIRAP were treated with GSH or GSNO 100, and 500 μM) for 1 h. Then, cell lysates were immunoprecipitated with anti-Flag antibody, followed by immunoblotting (IB) with anti-Flag a anti-Myc antibodies. (G) HEK293 cells transiently expressing Flag-tagged wild-type or Cys residue (113 or 216) replacement MyD88 together wi Myc-tagged TIRAP were treated with 500 μM SNAP for 1 h. Then, cell lysates were immunoprecipitated with anti-Flag antibody, followed immunoblotting with anti-Flag and anti-IRAK-1 antibodies.

time-dependent manner, although the restrictive effect continues for several hours (Fig. 5C).

NO suppresses acute-phase immune responses to LPS in vivo. To explore how NO regulation of MyD88-dependent signaling reflects innate immune or proinflammatory responses in vivo, we utilized a popular animal model of sepsis induced by i.p. administration of LPS. We first investigated the cytokine responses as the major hallmark of innate immune responses. MIP-2 is known as one of the early LPS-responsive genes, the mRNA expression of which indeed showed a rapid rise and reached a peak within 1 h after LPS stimulation in mouse peritoneal macrophages (Fig. 6A). In contrast, IL-6 is known as a late LPS-responsive gene, the expression of which showed a gradual rise and reached a peak more than 4 h after stimulation (Fig. 6A). We determined the amounts of MIP-2 and IL-6 produced in the abdominal cavity 2 h after LPS administration in wild-type, $eNOS^{-/-}$, and $iNOS^{-/-}$ mice. Interestingly, $eNOS^{-/-}$ mice exhibited the most intensive productio of MIP-2 (Fig. 6B). On the other hand, the most promine production of IL-6 was observed in $iNOS^{-/-}$ mice (Fig. 6C). contrast to these results, there was no significant difference the amounts of MIP-2 and IL-6 production when the flui were collected 12 h after LPS administration (data not shown Thus, eNOS and iNOS at least exert a suppressive effect early cytokine responses in vivo.

We further examined LPS-induced febrile response as hallmark of acute-phase responses of inflammation. LPS known to act as a pyrogen to induce TLR4-dependnet polyph sic fever (44). The major initiator of LPS fever is generat prostaglandin E2, which stimulates thermoregulatory neuro and elevates body core temperature (3). LPS can directly i duce prostaglandin E2 generation through the MyD88-depe dent signaling pathway (47). The first-phase febrile response $eNOS^{-/-}$ mice occurred significantly earlier than that in wil

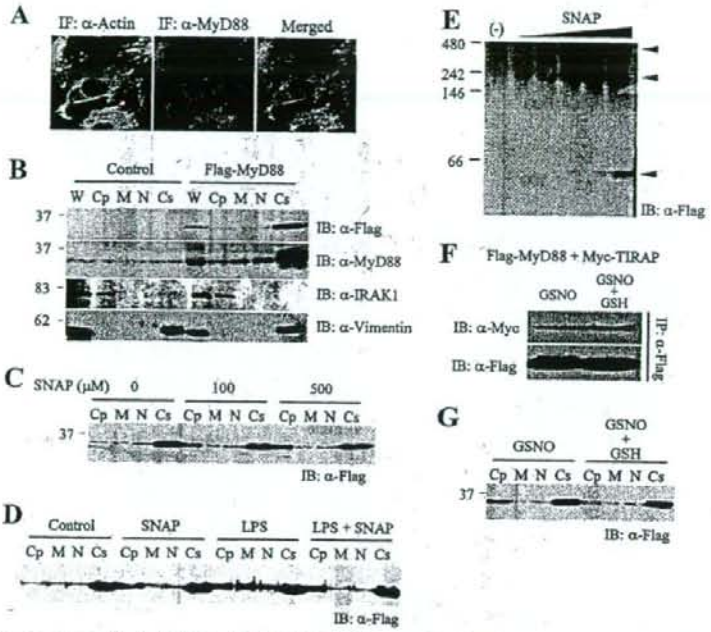

FIG. 4. Reverse of the suppressive effect of NO by GSH. (A) HAECs were fixed and stained immunofluorescently (IF) with anti-β-actin antibody (green, left), anti-MyD88 antibody (red, middle), and Hoechst33342 (blue, right). (B) Parental HEK293 cells and HEK293 cells stably expressing Flag-MyD88 were fractionated into the cytoplasm (Cp), cytoplasmic membrane (M), nucleus (N), and cytoskeleton (Cs). Whole-cell lysates (W) were also obtained. The fractions were assessed by immunoblotting (IB) with anti-Flag, anti-MyD88, anti-IRAK-1, and anti-vimentin antibodies. (C) HEK293 cells stably expressing Flag-MyD88 were treated with the indicated concentration of SNAP for 1 h and fractionated into each fraction. The fractions were assessed by immunoblotting with anti-Flag antibody. (D) 293-TLR4/MD2-CD14 cells stably expressing Flag-MyD88-GyrB were treated with or without 500μM SNAP for 1 h and then stimulated with 100 ng/ml LPS for 20 min. Cells were then fractionated into each fraction. The fractions were assessed by immunoblotting with anti-Flag antibody. (E) HEK293 cells stably expressing Flag-MyD88 were treated with or without SNAP (10, 50, 125, 250, and 500 μM) for 1 h. Then, cell lysates were assessed by blue native PAGE and immunoblotting with anti-Flag antibody. (F) HEK293 cells transiently expressing Flag-MyD88 and Myc-tagged TIRAP were treated with 500 μM GSNO for 1 h and then with or without 500 μM GSH for 15 min. Then, cell lysates were immunoprecipitated with anti-Flag antibody, followed by immunoblotting with anti-Flag and anti-Myc antibodies. (G) HEK293 cells stably expressing Flag-MyD88 were treated with the 500 μM GSNO for 1 h and then with or without 500 μM GSH for 15 min. The cells were fractionated into each fraction, followed by immunoblotting with anti-Flag antibody.

type or iNOS$^{-/-}$ mice (Fig. 6D), indicating that NO from eNOS suppresses the initiation of the response. However, eNOS deficiency did not alter the magnitude of febrile response compared with that for wild-type mice, suggesting that the suppressive effect of NO is not persistent. On the other hand, a transient decrease in fever was found in wild-type and eNOS$^{-/-}$ mice at about 70 min after LPS administration but not in iNOS$^{-/-}$ mice (Fig. 6D), indicating that NO from iNOS suppresses promotion of the response. Thus, these results suggest that NO generated from eNOS and iNOS exerts a suppressive effect on acute-phase inflammatory responses to LPS in vivo, probably through S nitrosylation.

DISCUSSION

Our findings imply that MyD88-dependent signaling events are affected by S nitrosylation, by which innate immune signal transduction might be reduced in living organisms. The effect of NO is transient and is restored by antioxidants or oxidoreductases, in which protein denitrosylation plays an important role. Although the physiological significance of such regulation of TLR signal transduction is unsettled, NO is likely to retard signaling cascades through S nitrosylation, by which rapid and precipitous signaling reactions may be initially or inductively relieved. Such an effect may reflect an adequate regulation of acute-phase inflammatory responses, leading to limitation of the degree of inflammation and resolution of inflammation.

We found that the suppressive effect of NO on TLR-mediated cellular responses was transient and degraded in a time-dependent manner (Fig. 5C). The specificity of NO regulation may be conferred by the spatial regulation of S nitrosylation within or between proteins and the stimulus-coupled temporal regulation through denitrosylation (14). Signal transduction by ligand-receptor interactions is thought to trigger denitrosylation, restoring substantial protein functions. For example, reduction of the functions of caspase-3 and IKKβ by S nitrosylation is restored by FasL-Fas interaction and TNF-α–TNFR interaction, respectively (30, 39). Thus, it is possible that TLR ligation-dependent protein denitrosylation also facilitates the restoration of NO suppression although the mechanism of denitrosylation has been poorly studied. Protein denitrosyla-

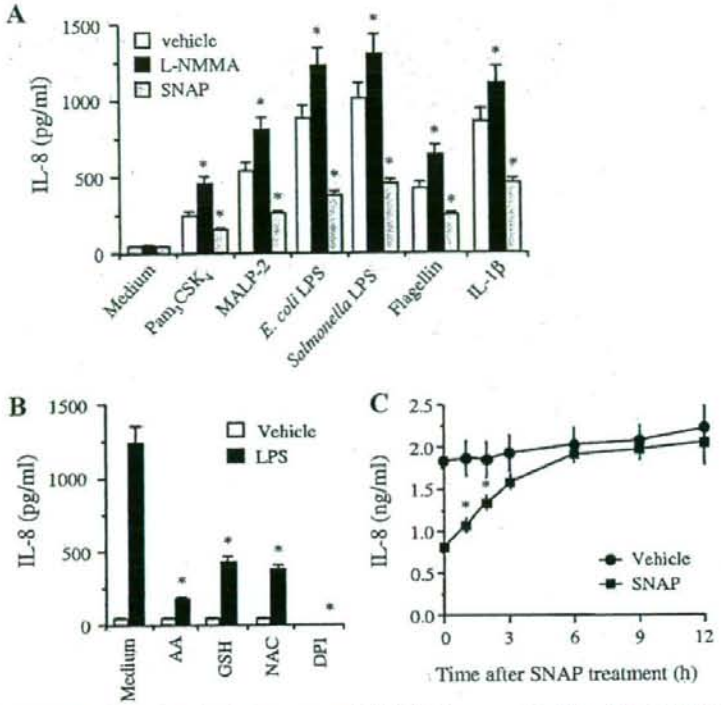

FIG. 5. NO reversibly suppresses TLR-mediated cellular responses. (A) HAECs pretreated with 1 mM L-NMMA for 12 h or 0.25 mM SNA for 1 h were stimulated with 1 μg/ml Pam_3CSK_4, 100 nM MALP-2, 10 ng/ml *E. coli* LPS, 10 ng/ml *Salmonella* LPS, 5 μg/ml flagellin, and 10 ng/ IL-1β for 3 h. Then, production of IL-8 was determined by ELISA. Each value is the mean ± SD ($n = 3$). *, $P < 0.01$ for comparison with t vehicle group. (B) HAECs were stimulated with 10 ng/ml *E. coli* LPS for 3 h in the presence or absence of 1 mM ascorbic acid (AA), 1 mM GS 1 mM NAC, or 20 μM DPI. Then production of IL-8 was determined by ELISA. Each value is the mean ± SD ($n = 3$). (*, $P < 0.01$ for comparis with the vehicle group). (C) HAECs were treated with 0.25 mM SNAP for 1 h and then at various times afterwards stimulated with 10 ng/ml *coli* LPS for 3 h. Then, production of IL-8 was determined by ELISA. Each value is the mean ± SD ($n = 3$). (*, $P < 0.01$ for comparison wi the vehicle group).

tion is catalyzed by antioxidants or oxidoreductases, including ascorbic acid, thioredoxin-thioredoxin reductase, superoxide dismutase GSH, and GSNO reductase (14, 15, 50, 53). S-nitrosylated MyD88 can be denitrosylated in the presence of ascorbic acid and GSH in vitro (Fig. 1C). Although it is still unclear how TLR ligation activates cellular redox activity, LPS has a potential to activate cellular redox activity and transition of GSH into GSNO (41). More details of TLR-mediated protein S nitrosylation and denitrosylation should be investigated in future studies.

TLR ligation can initiate recruitment of MyD88 to the receptor complex through TIR-TIR interaction. In the case of TLR2 and TLR4, the sorting adaptor TIRAP is essentially required to recruit MyD88 (23). MyD88 then dissociates from the receptor complex and recruits IRAK-1 (and IRAK-4) through death domain (DD)-DD interaction, inducing TRAF6-mediated signaling events and ubiquitin ligation to IRAK-1 or IκBα, followed by proteasomal degradation (1). Nevertheless, how MyD88 can be initially controlled to be recruited to TLRs has remained unclear. We found that a large part of cellular MyD88 existed in the cytoskeleton and associated with β-actin (Fig. 4A and B), wherein MyD88 formed a complex dissociated from IRAK-1 (Fig. 4B). Our finding suggests that MyD88 preferentially interacts with t cytoskeleton as an inactive form, followed by release into t cytoplasm and recruitment to TLRs after ligation-dependent a tin rearrangement. Indeed, inhibition of actin rearrangement cytochalasin D suppresses LPS-induced signal transduction a cytokine production (5). In addition, cytochalasin D also alte TIRAP recruitment to the cytoplasmic membrane (23). NO striction of MyD88 function may be achieved through disrupti of the protein complex and dissociation of MyD88 from the ac cytoskeleton to the cytoplasm (Fig. 4A to E). NO also reduces t interaction of MyD88 with TIRAP (Fig. 3). These effects m ultimately result in mitigated potential for the ligation-depende recruitment of MyD88 to TLRs.

We found that S nitrosylation of MyD88 plays some roles NO modulation of TLR signal transduction. Interesting eight of the nine cysteine residues of MyD88 are concentrat in the TIR domain, but the C-terminal DD contains no cy teine residue, suggesting that cysteine modification affec TIR-TIR interaction but not DD-DD interaction. Indeed, N attenuated the interaction of MyD88 with TIRAP but not th with IRAK-1 (Fig. 3). This result is supported by the resu found by Xiong et al. (52) showing that SNAP treatment d

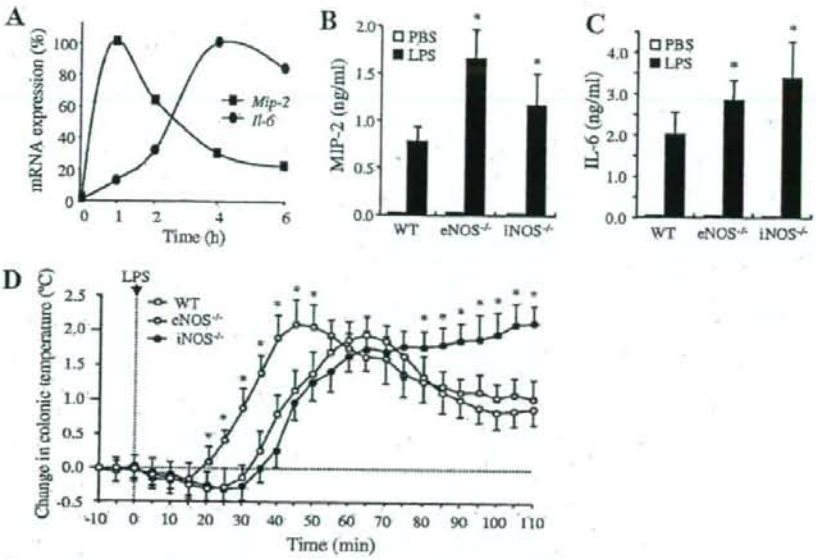

FIG. 6. Roles of eNOS and iNOS in early innate immune responses in vivo. (A) Peritoneal macrophages from wild-type mice were stimulated with 100 ng/ml LPS and 10 ng/ml gamma interferon for the indicated periods. Then, expression levels of mRNAs of *Mip-2* and *Il-6* were determined by quantitative PCR. Percent mRNA expression was calculated by taking the maximum values of mRNA levels of *Mip-2* and *Il-6* as 100%. (B, C) Wild-type (WT), eNOS$^{-/-}$, and iNOS$^{-/-}$ mice were i.p. treated with LPS. After 2 h, PBS was injected into the abdominal cavity and fluids were collected for measurement of the amounts of MIP-2 (B) and IL-6 (C) by ELISA. Each value is the mean ± SD ($n = 6$). (*, $P < 0.01$ for comparison with wild-type mice). (D) Wild-type, eNOS$^{-/-}$, and iNOS$^{-/-}$ mice were i.p. treated with LPS. The colonic temperature was monitored at 5-min intervals during a period of 10 min before and 120 min after LPS administration. Each value is the mean ± SD ($n = 6$). (*, $P < 0.01$ for comparison with wild-type mice).

not affect the interaction of MyD88 with IRAK-1 in mouse macrophages. Although S nitrosylation of the Cys216 residue of MyD88 may participate in the NO regulation of TLR signal transduction, it is likely that this modification does not have a dominant effect, because Cys216 was not essential for activation of downstream signaling (Fig. 1G). NO modification of Cys216 may yield a slight structural change in the base of the TIR domain, resulting in slightly reduced interaction with a counterpart TIR domain of TIRAP. Alternatively, NO may antagonize other reversible modifications, such as palmitoylation or disulfide bonding to a counterpart molecule, leading to transient impairment of MyD88 functioning. Also, other unknown mechanisms for MyD88 regulation may be negatively influenced by S nitrosylation.

We found that eNOS and iNOS differentially regulate LPS-induced acute-phase immune responses in vivo (Fig. 6). Although the amount of NO derived from eNOS is comparatively small, NO is steadily generated from endothelial cells as a vasodilatory gas that continually maintains an antiproliferative and antiapoptotic environment in vasculatures (16). Simultaneously, eNOS increases the amounts of cellular S-nitrosylated proteins and circulating NO donors by nitrosylating GSH and albumin (40). Such functions of NO from eNOS may systemically reduce cellular reactivity to a TLR stimulus to maintain a weak tolerance, which may lead to prevention of a rapid rise of inflammation. In contrast, NO from iNOS is generated in large quantities and exerts a strong antimicrobial action, although NO from eNOS also has an antimicrobial property (4, 29). The large amount of NO derived from iNOS is thought to disrupt cellular signaling cascades, resulting in anti-inflammatory or immunosuppressive effects. Such functions of NO from iNOS may regionally reduce cellular reactivity to TLR recognition of pathogens to initiate an inducible tolerance, which may transiently prevent promotion of excess inflammatory responses, although excess NO production ultimately results in nitrosative stress and apoptotic cell death (12, 26).

Our study proposes that TLR signal transduction involves an oxidative protein modification by NO and its redox regulation. NO may exert other effects, such as activation of cyclic-GMP-dependent signaling, on TLR signaling events, but such effects may not be dominant, at least in the acute-phase innate immune responses. Further investigations will be necessary to clarify more details about the relationship between such NO regulation and physiological or pathophysiological innate immune responses.

ACKNOWLEDGMENTS

We thank Margaret K. Offermann (Emory University School of Medicine) for providing DNA constructs of human MyD88 and TIRAP.

This work was supported by grants-in-aid for Scientific Research on Priority Areas (19041079 to T. Into) and for Young Scientists (B: 18791363 to T. Into), provided by the Ministry of Education, Culture, Sports, Science and Technology, Japan.

REFERENCES

1. **Akira, S., and K. Takeda.** 2004. Toll-like receptor signalling. Nat. Rev. Immunol. 4:499–511.

2. **Akira, S., S. Uematsu, and O. Takeuchi.** 2006. Pathogen recognition and innate immunity. Cell **124**:783–801.
3. **Blatteis, C. M., E. Sehic, and S. Li.** 2000. Pyrogen sensing and signaling: old views and new concepts. Clin. Infect. Dis. **31**:S168–177.
4. **Bogdan, C.** 2001. Nitric oxide and the immune response. Nat. Immunol. **2**:907–916.
5. **Dai, Q., and S. B. Pruett.** 2006. Ethanol suppresses LPS-induced Toll-like receptor 4 clustering, reorganization of the actin cytoskeleton, and associated TNF-α production. Alcohol Clin. Exp. Res. **30**:1436–1444.
6. **Dimmeler, S., J. Haendeler, M. Nehls, and A. M. Zeiher.** 1997. Suppression of apoptosis by nitric oxide via inhibition of interleukin-1β-converting enzyme (ICE)-like and cysteine protease protein (CPP)-32-like proteases. J. Exp. Med. **185**:601–607.
7. **Farrar, M. A., I. Alberol, and R. M. Perlmutter.** 1996. Activation of the Raf-1 kinase cascade by coumermycin-induced dimerization. Nature **383**:178–181.
8. **Forrester, M. T., M. W. Foster, and J. S. Stamler.** 2007. Assessment and application of the biotin switch technique for examining protein *S*-nitrosylation under conditions of pharmacologically induced oxidative stress. J. Biol. Chem. **282**:13977–13983.
9. **Forstermann, U., J. P. Boissel, and H. Kleinert.** 1998. Expressional control of the 'constitutive' isoforms of nitric oxide synthase (NOS I and NOS III). FASEB J. **12**:773–790.
10. **Ghosh, S., and M. Karin.** 2002. Missing pieces in the NF-κB puzzle. Cell **109**:S81–96.
11. **Häcker, H., V. Redecke, B. Blagoev, I. Kratchmarova, L. C. Hsu, G. G. Wang, M. P. Kamps, E. Raz, H. Wagner, G. Hacker, M. Mann, and M. Karin.** 2006. Specificity in Toll-like receptor signalling through distinct effector functions of TRAF3 and TRAF6. Nature **439**:204–207.
12. **Hara, M. R., N. Agrawal, S. F. Kim, M. B. Cascio, M. Fujimuro, Y. Ozeki, M. Takahashi, J. H. Cheah, S. K. Tankou, L. D. Hester, C. D. Ferris, S. D. Hayward, S. H. Snyder, and A. Sawa.** 2005. *S*-nitrosylated GAPDH initiates apoptotic cell death by nuclear translocation following Siah1 binding. Nat. Cell Biol. **7**:665–674.
13. **Hayden, M. S., A. P. West, and S. Ghosh.** 2006. NF-κB and the immune response. Oncogene **25**:6758–6780.
14. **Hess, D. T., A. Matsumoto, S. O. Kim, H. E. Marshall, and J. S. Stamler.** 2005. Protein *S*-nitrosylation: purview and parameters. Nat. Rev. Mol. Cell Biol. **6**:150–166.
15. **Hoffmann, J., J. Haendeler, A. M. Zeiher, and S. Dimmeler.** 2001. TNFα and oxLDL reduce protein *S*-nitrosylation in endothelial cells. J. Biol. Chem. **276**:41383–41387.
16. **Ignarro, L. J.** 2002. Nitric oxide as a unique signaling molecule in the vascular system: a historical overview. J. Physiol. Pharmacol. **53**:503–514.
17. **Into, T., J. Dohkan, M. Inomata, M. Nakashima, K. Shibata, and K. Matsushita.** 2007. Synthesis and characterization of a dipalmitoylated lipopeptide derived from paralogous lipoproteins of *Mycoplasma pneumoniae*. Infect. Immun. **75**:2253–2259.
18. **Into, T., Y. Kanno, J. Dohkan, M. Nakashima, M. Inomata, K. Shibata, C. J. Lowenstein, and K. Matsushita.** 2007. Pathogen recognition by Toll-like receptor 2 activates Weibel-Palade body exocytosis in human aortic endothelial cells. J. Biol. Chem. **282**:8134–8141.
19. **Into, T., and K. Shibata.** 2005. Apoptosis signal-regulating kinase 1-mediated sustained p38 mitogen-activated protein kinase activation regulates mycoplasmal lipoprotein- and staphylococcal peptidoglycan-triggered Toll-like receptor 2 signalling pathways. Cell. Microbiol. **7**:1305–1317.
20. **Iwasaki, A., and R. Medzhitov.** 2004. Toll-like receptor control of the adaptive immune responses. Nat. Immunol. **5**:987–995.
21. **Jaffrey, S. R., H. Erdjument-Bromage, C. D. Ferris, P. Tempst, and S. H. Snyder.** 2001. Protein *S*-nitrosylation: a physiological signal for neuronal nitric oxide. Nat. Cell Biol. **3**:193–197.
22. **Jaunin, F., K. Burns, J. Tschopp, T. E. Martin, and S. Fakan.** 1998. Ultrastructural distribution of the death-domain-containing MyD88 protein in HeLa cells. Exp. Cell Res. **243**:67–75.
23. **Kagan, J. C., and R. Medzhitov.** 2006. Phosphoinositide-mediated adaptor recruitment controls Toll-like receptor signaling. Cell **125**:943–955.
24. **Karin, M., and F. R. Greten.** 2005. NF-κB: linking inflammation and immunity to cancer development and progression. Nat. Rev. Immunol. **5**:749–759.
25. **Kelleher, Z. T., A. Matsumoto, J. S. Stamler, and H. E. Marshall.** 2007. NOS2 regulation of NF-κB by *S*-nitrosylation of p65. J. Biol. Chem. **282**: 30667–30672.
26. **Kim, K. M., P. K. Kim, Y. G. Kwon, S. K. Bai, W. D. Nam, and Y. M. Kim.** 2002. Regulation of apoptosis by nitrosative stress. J. Biochem. Mol. Biol. **35**:127–133.
27. **Laroux, F. S., X. Romero, L. Wetzler, P. Engel, and C. Terhorst.** 2005. MyD88 controls phagocyte NADPH oxidase function and killing of gram-negative bacteria. J. Immunol. **175**:5596–5600.
28. **Lawrence, T., M. Bebien, G. Y. Liu, V. Nizet, and M. Karin.** 2005. IKKα limits macrophage NF-κB activation and contributes to the resolution of inflammation. Nature **434**:1138–1143.
29. **MacMicking, J., Q. W. Xie, and C. Nathan.** 1997. Nitric oxide and macrophage function. Annu. Rev. Immunol. **15**:323–350.
30. **Mannick, J. B., A. Hausladen, L. Liu, D. T. Hess, M. Zeng, Q. X. Miao, Kane, A. J. Gow, and J. S. Stamler.** 1999. Fas-induced caspase denitro tion. Science **284**:651–654.
31. **Mannick, J. B., C. Schonhoff, N. Papeta, P. Ghafourifar, M. Szibor, K. F and B. Gaston.** 2001. *S*-Nitrosylation of mitochondrial caspases. J. Cell **154**:1111–1116.
32. **Marshall, H. E., D. T. Hess, and J. S. Stamler.** 2004. *S*-nitrosylation: iological regulation of NF-κB. Proc. Natl. Acad. Sci. USA **101**:8841–8
33. **Marshall, H. E., and J. S. Stamler.** 2001. Inhibition of NF-κB by *S*-nit lation. Biochemistry **40**:1688–1693.
34. **Matsuzawa, A., K. Saegusa, T. Noguchi, C. Sadamitsu, H. Nishito Nagai, S. Koyasu, K. Matsumoto, K. Takeda, and H. Ichijo.** 2005. dependent activation of the TRAF6-ASK1-p38 pathway is selectivel quired for TLR4-mediated innate immunity. Nat. Immunol. **6**:587–59
35. **Medzhitov, R., P. Preston-Hurlburt, and C. A. Janeway, Jr.** 1997. A h homologue of the Drosophila Toll protein signals activation of ada immunity. Nature **388**:394–397.
36. **Medzhitov, R., P. Preston-Hurlburt, E. Kopp, A. Stadlen, C. Chen, S. G and C. A. Janeway, Jr.** 1998. MyD88 is an adaptor protein in the hTol receptor family signaling pathways. Mol. Cell **2**:253–258.
37. **Miggin, S. M., E. Palsson-McDermott, A. Dunne, C. Jefferies, E. Pint K. Banahan, C. Murphy, P. Moynagh, M. Yamamoto, S. Akira, N. Rot D. Golenbock, K. A. Fitzgerald, and L. A. O'Neill.** 2007. NF-κB activati the Toll-IL-1 receptor domain protein MyD88 adapter-like is regulat caspase-1. Proc. Natl. Acad. Sci. USA **104**:3372–3377.
38. **Park, H. S., J. W. Yu, J. H. Cho, M. S. Kim, S. H. Huh, K. Ryoo, and Choi.** 2004. Inhibition of apoptosis signal-regulating kinase 1 by nitric through a thiol redox mechanism. J. Biol. Chem. **279**:7584–7590.
39. **Reynaert, N. L., K. Ckless, S. H. Korn, N. Vos, A. S. Guala, E. F. Wo A. van der Vliet, and Y. M. Janssen-Heininger.** 2004. Nitric oxide rep inhibitory κB kinase through *S*-nitrosylation. Proc. Natl. Acad. Sci. **101**:8945–8950.
40. **Richardson, G., and N. Benjamin.** 2002. Potential therapeutic uses nitrosothiols. Clin. Sci. (London) **102**:99–105.
41. **Rubin, D. B., G. Reznik, E. A. Weiss, and P. R. Young.** 2000. Non-p thiols flux to *S*-nitrosothiols in endothelial cells: an LPS redox signal. **14**:200–207.
42. **Stamler, J. S., S. Lamas, and F. C. Fang.** 2001. Nitrosylation. The prot redox-based signaling mechanism. Cell **106**:675–683.
43. **Stamler, J. S., D. I. Simon, J. A. Osborne, M. E. Mullins, O. Jara Michel, D. J. Singel, and J. Loscalzo.** 1992. *S*-nitrosylation of protein nitric oxide: synthesis and characterization of biologically active compo Proc. Natl. Acad. Sci. USA **89**:444–448.
44. **Steiner, A. A., S. Chakravarty, A. Y. Rudaya, M. Herkenham, and Romanovsky.** 2006. Bacterial lipopolysaccharide fever is initiated via like receptor 4 on hematopoietic cells. Blood **107**:4000–4002.
45. **Steiner, A. A., A. Y. Rudaya, A. I. Ivanov, and A. A. Romanovsky.** Febrigenic signaling to the brain does not involve nitric oxide. Br. J. macol. **141**:1204–1213.
46. **Thoma-Uszynski, S., S. Stenger, O. Takeuchi, M. T. Ochoa, M. Engele Sieling, P. F. Barnes, M. Rollinghoff, P. L. Bolcskei, M. Wagner, S. M. V. Norgard, J. T. Belisle, P. J. Godowski, B. R. Bloom, and R. L. M** 2001. Induction of direct antimicrobial activity through mammalian To receptors. Science **291**:1544–1547.
47. **Uematsu, S., M. Matsumoto, K. Takeda, and S. Akira.** 2002. Lipopo charide-dependent prostaglandin E(2) production is regulated by the thione-dependent prostaglandin E(2) synthase gene induced by the To receptor 4/MyD88/NF-IL6 pathway. J. Immunol. **168**:5811–5816.
48. **Vulcano, M., S. Dusi, D. Lissandrini, R. Badolato, P. Mazzi, E. Ribo Borroni, A. Calleri, M. Donini, A. Plebani, L. Notarangelo, T. Musso, Sozzani.** 2004. Toll receptor-mediated regulation of NADPH oxid human dendritic cells. J. Immunol. **173**:5749–5756.
49. **Wang, W., A. Mitra, B. Poole, S. Falk, M. S. Lucia, S. Tayal, and R. Sc** 2004. Endothelial nitric oxide synthase-deficient mice exhibit increase ceptibility to endotoxin-induced acute renal failure. Am. J. Physiol. Physiol. **287**:F1044–F1048.
50. **West, M. B., B. G. Hill, Y. T. Xuan, and A. Bhatnagar.** 2006. P glutathiolation by nitric oxide: an intracellular mechanism regulating protein modification. FASEB J. **20**:1715–1717.
51. **Woronicz, J. D., X. Gao, Z. Cao, M. Rothe, and D. V. Goeddel.** 199 kinase-β: NF-κB activation and complex formation with IκB kinase- NIK. Science **278**:866–869.
52. **Xiong, H., C. Zhu, F. Li, R. Hegazi, K. He, M. Babyatsky, A. J. Baue S. E. Plevy.** 2004. Inhibition of interleukin-12 p40 transcription and N activation by nitric oxide in murine macrophages and dendritic cells. J Chem. **279**:10776–10783.
53. **Yamawaki, H., J. Haendeler, and B. C. Berk.** 2003. Thioredoxin: regulator of cardiovascular homeostasis. Circ. Res. **93**:1029–1033.

Cardiovascular Research (2008) 77, 221–230
doi:10.1093/cvr/cvm049

Nitric oxide regulates vascular calcification by interfering with TGF-β signalling

Yosuke Kanno[1,2]*, Takeshi Into[1], Charles J. Lowenstein[3], and Kenji Matsushita[1]*

[1]*Department of Oral Disease Research, National Center for Geriatrics and Gerontology, 36-3 Gengo, Morioka-cho, Obu, Aichi 474-8511, Japan;* [2]*Department of Clinical Pathological Biochemistry, Faculty of Pharmaceutical Science, D.W.C.L.A., Kyo-tanabe, Kyoto 610-0395, Japan; and* [3]*The Johns Hopkins University School of Medicine, Baltimore, MD 21205, USA*

Received 27 March 2007; revised 3 October 2007; accepted 21 October 2007; online publish-ahead-of-print 25 October 2007

Time for primary review: 19 days

KEYWORDS
Atherosclerosis;
Vascular calcification;
Vascular ageing;
Diabetes mellitus

Aims Vascular calcification often occurs with advancing age, atherosclerosis, and metabolic disorders such as diabetes mellitus and end-stage renal disease. Vascular calcification is associated with cardiovascular events and increased mortality. Nitric oxide (NO) is crucial for maintaining vascular function, but little is known about how NO affects vascular calcification. The aim of this study was to examine the effect of NO on vascular calcification.

Methods and results In this study, we examined the inhibitory effects of NO on calcification of murine vascular smooth muscle cells (VSMCs) *in vitro*. We measured calcium concentration, alizarin red staining, and alkaline phosphatase activity to examine the effect of NO on calcification of VSMCs and differentiation of VSMCs into osteoblastic cells. We also determined gene expression and levels of phosphorylation of Smad2/3 by RT–PCR and western blotting. NO inhibited calcification of VSMCs and differentiation of VSMCs into osteoblastic cells. An inhibitor of cyclic guanosine monophosphate (cGMP)-dependent protein kinase restored the inhibition by NO of osteoblastic differentiation and calcification of VSMCs. NO inhibited transforming growth factor-β (TGF-β)-induced phosphorylation of Smad2/3 and expression of TGF-β-induced genes such as plasminogen activator inhibitor-1. In addition, NO inhibited expression of the TGF-β receptor ALK5.

Conclusion Our data show that NO prevents differentiation of VSMCs into osteoblastic cells by inhibiting TGF-β signalling through a cGMP-dependent pathway. Our findings suggest that NO may play a beneficial role in atherogenesis in part by limiting vascular calcification.

Introduction

Vascular calcification occurs in many diseases, including atherosclerosis, diabetes, and uremia.[1–3] Deposition of calcification in arteries diminishes arterial wall elasticity, obstructs blood flow, and can lead to heart attacks and stroke.[4] The presence of calcium deposits in the vessel wall is indicative of advanced atherosclerosis, and the extent of coronary calcification adds independent prognostic significance to conventional risk factors for coronary artery disease. Vascular calcification is a major independent predictor of cardiovascular morbidity and mortality.[5]

Vascular calcification has been considered to be an organized, regulated process similar to mineralization in bone tissue.[6,7] Specific bone-associated proteins such as matrix Gla protein are constitutively expressed at low levels in the healthy vessel, and their expression increases during vascular calcification.[8,9] Moreover, the expression of a number of bone-associated proteins such as osteopontin normally absent in the vessel wall is also increased in the calcified vessel wall.[9]

Vascular smooth muscle cells (VSMCs) play a major role in vascular calcification.[10] VSMCs contribute to the development of an atherosclerotic lesion by migration, proliferation, and secretion of matrix components.[11,12] VSMCs also express many of the calcification-regulating proteins commonly found in bone.[8–9,13] These proteins have calcium and apatite binding properties, and accumulate in areas of vascular calcification. Among them, transforming growth factor-β (TGF-β) is a key factor in vascular calcification. TGF-β is present in calcified aortic valves,[14] and regulates vascular calcification and osteoblastic differentiation of VSMCs.[6,15]

Nitric oxide (NO) is a messenger molecule produced by the NO synthase (NOS) isoforms neuronal NOS (nNOS, or NOS1), inducible NOS (iNOS, or NOS2), and endothelial NOS (eNOS, or NOS3).[16,17] All three NOS isoforms can be found in the vasculature – NOS1 in nerve fibbers in the adventitia,

* Corresponding author. Tel: +81 0774 65 8629; fax: +81 0774 65 8479.
E-mail address: ykanno@dwc.doshisha.ac.jp (Y.K.). Tel: +81 562 46 2311 (ext. 5401); fax:+81 562 46 8479. *E-mail address*: kmatsu30@nils.go.jp (K.M.)

NOS2 in VSMCs and in infiltrating macrophages during vascular inflammation, and NOS3 in endothelial cells – and NO has a variety of effects upon vascular cells. NO produced in the endothelium by eNOS activates smooth muscle cell relaxation and vasodilation by binding to soluble guanylate cyclase, resulting in cyclic guanosine monophosphate (cGMP) production and the activation of signal transduction pathways. NO also inhibits smooth muscle cell migration and proliferation.[18,19] NO may also affect vascular calcification. However, the effect of NO on vascular calcification is not understood.

Although TGF-β induces vascular calcification, the regulatory mechanism of vascular calcification is not well clarified. We hypothesized that NO inhibits vascular calcification by regulating TGF-β signalling. Here we show that NO regulates vascular calcification in part by interfering with TGF-β signalling.

Methods

All experiments were performed in accordance with the Guide for the Care and Use of Laboratory Animals published by the US National Institutes of Health.

Reagents

Recombinant human TGF-β_1 and 8-bromo-cGMP were from Calbiochem (Daemsradt USA). The NO donor DETA-NONOate was from Cayman Chemical Co. (Ann Arbor, MI, USA). The NOS inhibitor aminoguanidine hemisulphate (AG) was purchased from Sigma-Aldrich (St Louis, MO, USA). The guanylate cyclase inhibitor ODQ was from Wako Pure Chemical (Osaka, Japan). The protein kinase G (PKG) inhibitor KT5823 was from Sigma-Aldrich.

Cell culture and analysis of vascular smooth muscle cell calcification

VSMCs were obtained from the thoracic aorta of C57BL/6J mice.[20] Induction of calcification of VSMCs was performed by a procedure of Tintut *et al.*[21] with minor modifications. VSMCs were grown in Dulbecco's modified Eagle's medium (Sigma-Aldrich) containing 10% heat-inactivated foetal bovine serum and supplemented with 1 mM sodium pyruvate, 100 units/ml penicillin, and 100 units/mL streptomycin. After 4 days, the media was replaced with calcification media (media supplemented with 5 mM β-glycerophosphate and 4 mM $CaCl_2$) to permit maximal mineralization. The calcification media were changed every 3–4 days. To examine the effect of NO on VSMC calcification, VSMCs were grown in calcification media with DETA-NONOate for 14 days. To become 10 μM, we added DETA NONOate at intervals of 20 h.

To determine the degree of mineralization, calcium concentration in the cells was measured by Calcium Assay Kit (BioAssay Systems). After 14 days in culture, cells were then washed, and proteins in cells were extracted with a lysis buffer (10 mM Tris-HCl, pH 7.5, 0.1% Triton X-100). A phenolsulphonephthalein dye in the kit forms a very stable blue coloured complex specifically with free calcium. The intensity of the colour, measured at 612 nm, is directly proportional to the calcium concentration in the sample.

Alizarin red staining

Calcified VSMCs were stained with alizarin red S (Kanto Chemical, Japan). After washing, cultures were fixed with 4% paraformaldehyde in PBS for 15 min, and then stained with 2% alizarin red S in H_2O for 30 min at room temperature. After staining, cultures were washed three times.

Cell viability assays

Cell viability was assessed as a function of NADH content using a Te raColor ONE [5 mM (2-(2-methoxy-4-nytrophenyl)-3-(4-nitrophenyl 5-(2,4-disulphophenyl)-2*H*-tetrazolium, monosodium salt); 0.2 m 1-methoxy-5-metylphenazinium methylsulphate; and 150 mM NaCl based assay according to the manufacturer's instructions (Seikagak Inc., Nihonbashi, Tokyo, Japan). VSMCs were grown in calcificatic media with DETA-NONOate for 14 days. After 14 days, cell viabili was evaluated using TetraColor ONE (Seikagaku Corp.). Finall 10 μL of TetraColor ONE solution was added to each well, and t cells were incubated for 1.5 h. A well for the negative control w prepared as described above without cells. The absorbance each well was then determined at a wavelength of 450 nm.

Measurement of alkaline phosphatase activity

VSMCs were seeded at a density of 4×10^5 cells/well on six-w plates. After 14 days in culture, cells were then washed, and pr teins in cells were extracted with a lysis buffer (10 mM Tris-H pH 7.5, 0.1% Triton X-100). Alkaline phosphatase (ALP) activi was determined using *p*-nitro phenyl phosphate (Sigma-Aldrich) a substrate. Protein concentration of extracts was determined BCA protein assay kit (Pierce) using bovine serum albumin as standard.

Inducible nitric oxide synthase and endothelial nitric oxide synthase overexpressing vascular smooth muscle cells

VSMCs were transfected with iNOS (mouse) and eNOS (bovir plasmid (pcDNA 3.1/His 'A' vector) by using Lipofectamine 200 From the second day after the transfection, iNOS or eNOS empty vector-transfected cells were selected with 200 μg/ G418 for 4 weeks. These VSMCs were cultured as described abov

Reverse transcription-polymerase chain reaction

Total RNA was isolated from VSMCs using Isogen (Nippon Ge Japan) and was reverse-transcribed using MMLV reverse transcr tase (GIBCO BRL). The transcripts were amplified by PCR using *Taq* (TaKaRa, Japan). The following primers were synthesize PAI-1 sense, AAAGGTATGATCAATGACTTACTGG; PAI-1 antisen TCAAAGGGTGCAGCGATGAACATGC; ALK1 sense, TGACTTTCTGC GAGGCAGA; ALK1 antisense, CGACTCAAAGCAGTCTGTGC; AL sense, ATCCATCACTAGATCGCCCT; ALK5 antisense, CGATGGAT GAAGGTACAAGA; type I collagen sense, ATCCCCATGACTGTCTAT type I collagen antisense, CAAATAAGTGACCATCGCCA; osteocal (OC) sense, TGCGCTCTGTCTCTCTGACC; OC antisense, CTGT CATCCATACTTGCAGG; matrix Gla protein 2 (MGP2) sen ACCACGTCCCAGCTTCTAGC; and MGP2 antisense, GCTCTGCGATG GAGGTACTG; PCR amplification of cDNA for 35 cycles was at 9 denaturation (60 s), 60°C annealing (60 s), and 72°C extens (60 s). Following PCR amplifications, the amplified cDNAs w further extended by additional incubation at 72°C for 10 min. equal amount of each reaction was fractionated on 1% agarose in 1 × TAE buffer, and then the agarose gel was soaked in 1 × buffer containing ethidium bromide for 15 min by gentle agitati The amplified cDNA fragments in the agarose gel were then visu ized on a UV transilluminator and photographed.

Western blot analysis for Smad2/3

VSMCs grown in a six-well plate were washed twice with ice-c PBS; lysed with 62.5 mM Tris-HCl (pH 6.8) containing 2% SDS, glycerol, and 50 mM DTT (an SDS sample buffer) in the prese of inhibitor cocktails of proteases (Sigma-Aldrich); and boiled 10 min. The lysates were centrifuged at 14 000 rpm for 10 m and the resulting supernatants containing cytosolic and membr proteins were collected. Proteins in the supernatant were separa

by electrophoresis on 10% SDS-polyacrylamide gels and transferred to a nitrocellulose membrane. The membrane was incubated at 4°C overnight with polyclonal antibody to Smad2/3 or antibody to phospho-Smad2/3 and then with peroxidase-conjugated antibody to rabbit IgG. Immunoreactive proteins were detected using ECL detection reagents (Amersham Pharmacia Biotech).

Statistical analysis

All data are expressed as mean ± SEM. The significance of the effect of each treatment ($P < 0.05$) was determined by analysis of variance (ANOVA) followed by the Student Newman-Keuls test.

Results

Nitric oxide inhibits vascular smooth muscle cell calcification

To explore the effect of NO on vascular calcification, we incubated VSMCs from murine aorta in DMEM media supplemented with 5 mM β-glycerophosphate and 4 mM $CaCl_2$ (calcification media) in the presence or absence of DETA-NONOate for 14 days, and then the amount of calcification in cells were measured by alizarin red staining. Calcification media induced mineralization of VSMCs. However, the NO donor inhibits VSMC calcification (*Figure 1A* and *B*). The NO donor did not affect on the cell viability (*Figure 1C*).

To explore the role of NO in the regulation of vascular calcification, we first measured NOS mRNA expression in VSMCs and calcified VSMCs by RT-PCR. VSMCs expressed mRNAs of eNOS and iNOS, and the expression levels were increased in calcified VSMCs (*Figure 1D*). Calcified VSMCs also expressed nNOS mRNA. We next treated calcifying VSMCs with an NO inhibitor AG for 14 days and measured calcification. AG increased VSMC calcification (*Figure 1E*). Moreover, we examined the effect of iNOS and eNOS on VSMCs calcification by transfection of iNOS and eNOS plasmid (*Figure 1F*). iNOS and eNOS overexpression inhibited VSMC calcification (*Figure 1G*). These data suggest NO regulates vascular calcification.

Nitric oxide inhibits osteoblastic differentiation of vascular smooth muscle cells

We next examined the effect of NO on osteoblastic differentiation of VSMCs. ALP, one of the phenotypic markers of osteoblasts, is thought to be essential to bone mineralization.[22] Increased ALP activity was observed in calcified matrix vesicles of smooth muscle cells. Therefore, we examined the effect of NO on ALP activity in calcifying VSMCs. ALP activity was strongly detected in calcifying VSMCs. The NO donor inhibits ALP activity in calcifying VSMCs (*Figure 2A*). We also showed that the NO donor inhibits expression of other osteoblastic marker, type I collagen, OC, and MGP2 (*Figure 2B*). We next treated calcifying VSMCs with an NO inhibitor AG for 14 days and measured ALP activity. AG increased ALP activity of VSMC (*Figure 2C*). Moreover, we examined the effect of iNOS and eNOS on osteoblastic differentiation by transfection of iNOS and eNOS plasmid (*Figure 1F*). iNOS and eNOS overexpression inhibited osteoblastic differentiation of VSMCs (*Figure 2D*). These data suggest NO regulates osteoblastic differentiation of VSMCs.

Nitric oxide/cGMP/protein kinase G signalling pathway mediates vascular smooth muscle cell calcification

To determine whether or not NO inhibits vascular calcification through a cGMP pathway, we examined the effect of the guanylate cyclase inhibitor ODQ and the PKG inhibitor KT5823 on VSMCs calcification treated with NO. ODQ blocked the inhibitory effect of NO on VSMC calcification (*Figure 3A*). KT5823 also blocked the inhibitory effect of NO on VSMC calcification (*Figure 3B*). Furthermore, ODQ and KT5823 reversed the inhibitory effect of NO on osteoblastic differentiation (*Figure 3C* and *D*). ODQ and KT5823 increased osteoblastic differentiation in the absence of NO donor. However, ODQ and KT5823 did not increase VSMC calcification in the absence of NO donor. Then, we examined the effects of a cGMP analogue 8-bromo-cGMP on vascular calcification and osteoblastic differentiation of VSMC. Treatment with 8-bromo-cGMP inhibited VSMC calcification (*Figure 3E*). The cGMP analogue also inhibited ALP activity in calcifying VSMCs (*Figure 3F*).

Nitric oxide regulates transforming growth factor-β signalling in vascular smooth muscle cells

TGF-β regulates vascular calcification and osteoblastic differentiation of VSMCs.[6,15] Therefore, we explored the effect of NO on TGF-β signalling in VSMCs. We first examined the expression of TGF-β mRNA in calcified VSMCs by RT-PCR. Increased expression of TGF-β was observed in calcified VSMCs (*Figure 4A*). A neutralizing antibody to TGF-β inhibited VSMC calcification and osteoblastic differentiation (*Figure 4B–D*). We also examined the effect of NO on TGF-β-induced osteoblastic differentiation of VSMCs. The NO donor markedly reduced TGF-β-induced ALP activity in VSMCs (*Figure 4E*). On the other hand, TGF-β did not induce VSMC calcification in the absence of calcification media.

We next investigated whether NO affects TGF-β signalling in calcifying VSMCs. TGF-β activates a heteromeric complex of type I and type II transmembrane serine/threonine kinase receptors ALK-1 and ALK-5.[23] ALK5 activation induces phosphorylation of Smad2/3.[24] Therefore, we examined the effect of NO on Smad2/3 phosphorylation in calcifying VSMCs. The NO donor blocked TGF-β-induced phosphorylation of Smad2/3 (*Figure 5*). We also examined the effect of NO on TGF-β gene expression and its production. However, NO did not affect mRNA levels of TGF-β and TGF-β protein from calcified VSMCs (see Supplementary material online, Data 1 and 2), indicating that NO does not decrease phosphorylation of Smad2/3 by inhibiting TGF-β expression. We also investigated the effect of NO on ALK1 and ALK5 mRNA levels in calcifying VSMCs. NO markedly reduced ALK5 mRNA levels. However, NO did not reduce ALK1 mRNA (*Figure 6A*). We also investigated the effect of NO on the plasminogen activator inhibitor-1 (PAI-1) gene expression by RT-PCR, because ALK5 activates PAI-1 gene expression. NO markedly reduced mRNA expression of PAI-1 (*Figure 6B*). Moreover, we investigated the effect of KT5823 on the ALK5 and the PAI-1 gene expression treated with NO. KT5823 reversed the inhibitory effect of NO on the ALK5 and the PAI-1 gene expression (*Figure 6C*). These results suggest that NO inhibits VSMC calcification and

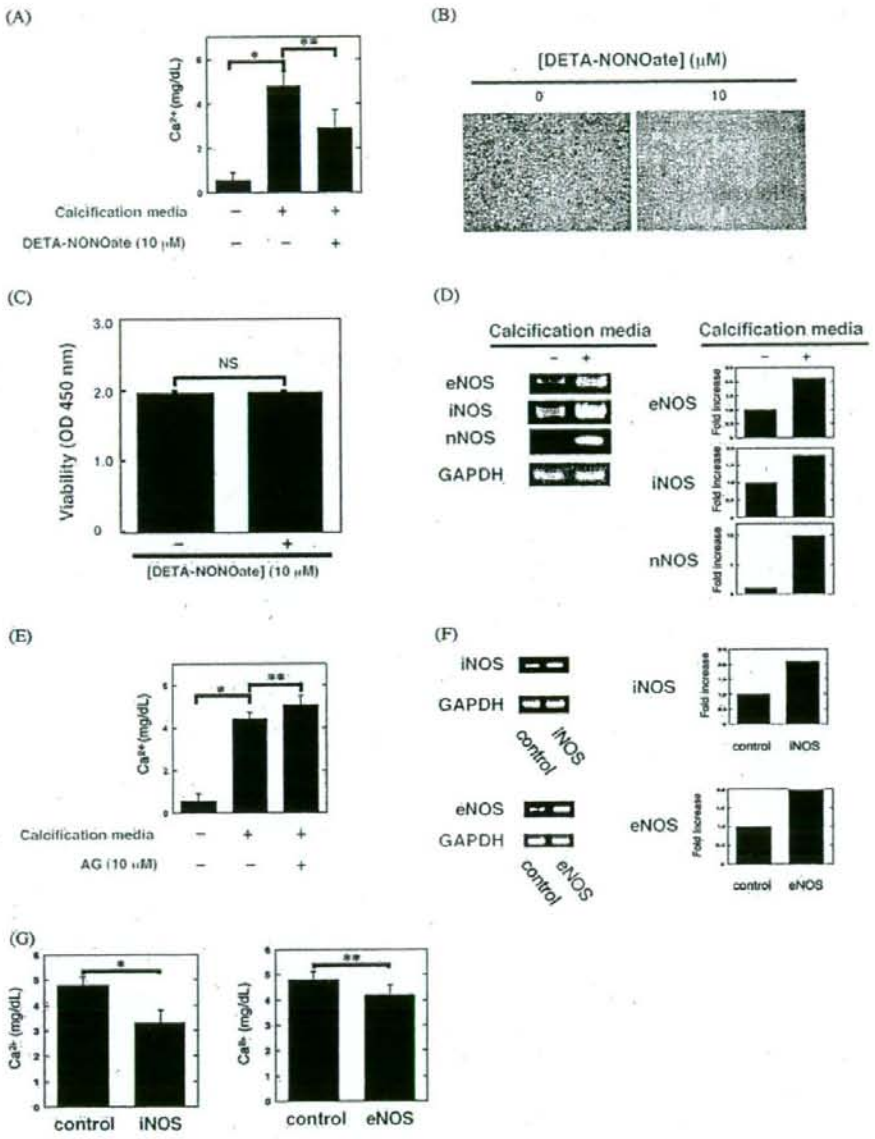

Figure 1 Nitric oxide (NO) inhibits vascular smooth muscle cell (VSMC) calcification. (*A*) VSMCs were grown with calcification media for 14 days in the sence or absence of 10 μM DETA-NONOate. Then, calcium concentration in the cells was measured as described in Methods section ($n = 5$–$6 \pm$ SEM, $^*P <$ $^{**}P < 0.05$). (*B*) Photomicrographs of Alizarin red staining of calcifying VSMCs treated with or without DETA-NONOate. (*C*) Effect of NO on viability of VS VSMCs were grown in calcification media with 10 μM DETA-NONOate for 14 days. Then the cell viability was assessed as a function of NADH content usi TetraColor ONE ($n = 3 \pm$ SEM). (*D*) Calcified VSMCs expressed eNOS, iNOS and nNOS. NOS expression in calcified VSMCs was measured by RT-PCR. Sir results were obtained with three additional and different samples. (*E*) NOS inhibitor increases VSMC calcification. VSMCs were grown in calcification m with an NOS inhibitor aminoguanidine hemisulphate (AG) for 14 days. Then, calcium concentration in the cells was measured as described in Met section ($n = 5$–$6 \pm$ SEM, $^*P < 0.01$, $^{**}P < 0.05$). (*F*) Transfection of iNOS and eNOS plasmid significantly increased iNOS and eNOS expression, measure RT-PCR. (*G*) NOS overexpression inhibits calcification of VSMCs. VSMCs were transfected with iNOS and eNOS plasmid. Then, VSMCs were grown with calci tion media for 14 days, and calcium concentration in the cells was measured as described in Methods section ($n = 5$–$6 \pm$ SEM, $^*P < 0.01$, $^{**}P < 0.05$).

osteoblastic differentiation of VSMCs by regulating TGF-β signalling.

Discussion

The major finding of this study is that NO inhibits vascular calcification by interfering with TGF-β signalling.

Nitric oxide inhibits vascular calcification

We found that NO inhibited VSMC calcification and ost blastic differentiation of VSMCs. NO inhibited an incre of ALP activity and other osteoblastic marker in calcify VSMCs. ALP is an enzyme that has been shown to be imp ant for matrix mineralization.[22] Osteoblasts increase

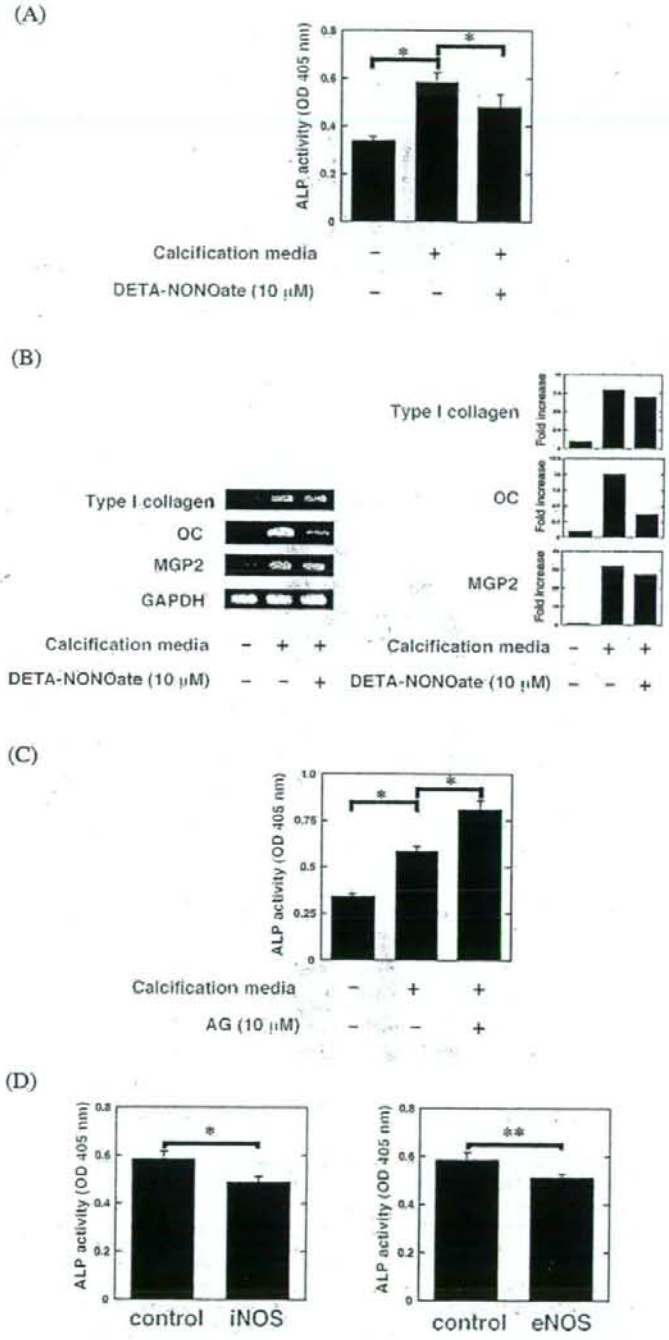

Figure 2 Nitric oxide (NO) inhibits osteoblastic differentiation of vascular smooth muscle cells (VSMCs). (*A*) NO inhibits increasing ALP activity in calcifying VSMCs. VSMCs were grown in calcification media with 10 μM DETA-NONOate for 14 days, and ALP activity at OD 405 nm was measured ($n = 6 \pm$ SEM, $^*P < 0.01$.). (*B*) NO inhibits expression of osteoblastic marker in calcifying VSMCs. VSMCs were grown in calcification media with 10 μM DETA-NONOate for 14 days, and expression of type I collagen, osteocalcin (OC) and matrix Gla protein 2 (MGP2) in calcified VSMCs was measured by RT-PCR. Similar results were obtained with three additional and different samples. (*C*) NOS inhibitor increases VSMC calcification. VSMCs were grown in calcification media with an NOS inhibitor aminoguanidine hemisulphate (AG) for 14 days, and ALP activity at OD 405 nm was measured ($n = 5$–$6 \pm$ SEM, $^*P < 0.01$, $^{**}P < 0.05$). (*D*) NOS overexpression inhibits osteoblastic differentiation of VSMCs. VSMCs were transfected with iNOS and eNOS plasmid. VSMCs were grown in calcification media for 14 days, and ALP activity at OD 405 nm was measured ($n = 6 \pm$ SEM, $^*P < 0.01$, $^{**}P < 0.05$).

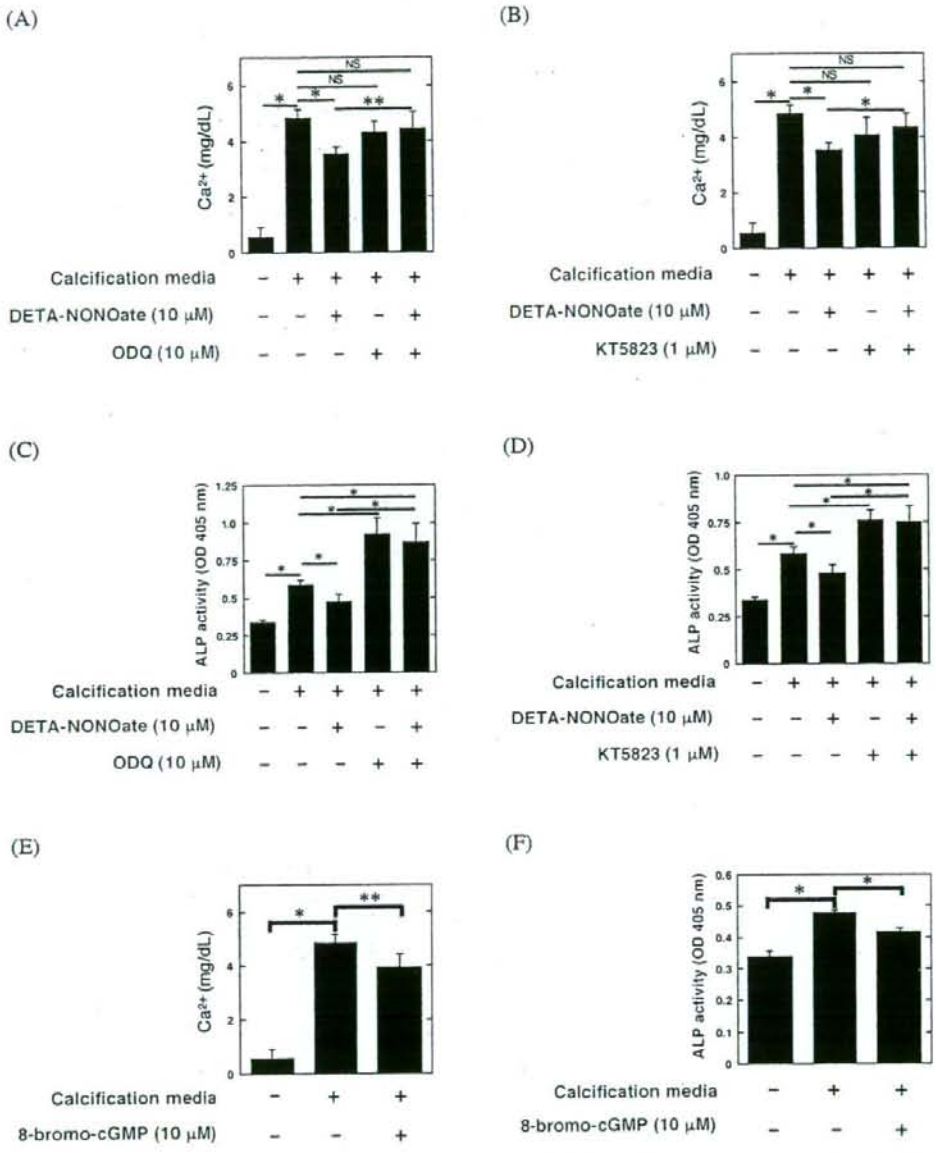

Figure 3 Nitric oxide (NO)-cGMP signalling pathway mediates vascular smooth muscle cell (VSMC) calcification. (*A*) Guanylate cyclase inhibitor ODQ blocks N inhibition of VSMC calcification. VSMCs were grown in calcification media with 10 μM DETA-NONOate for 14 days in the presence or absence of ODQ. Then, calciu concentration in the cells was measured as described in Methods section ($n = 4$–$6 \pm$ SEM, $^*P < 0.01$, $^{**}P < 0.05$). (*B*) The PKG inhibitor KT5823 blocks NO inh bition of VSMC calcification. VSMCs were grown in calcification media with DETA-NONOate for 14 days in the presence or absence of KT5823. Mineralization w measured as above ($n = 4$–$6 \pm$ SEM, $^*P < 0.01$). (*C*) ODQ blocks NO inhibition of VSMC osteoblastic differentiation. VSMCs were grown in calcification media wi 10 μM DETA-NONOate for 14 days in the presence or absence of ODQ, and ALP activity at OD 405 nm was measured ($n = 6 \pm$ SEM, $^*P < 0.01$). (*D*) KT5823 blocks N inhibition of VSMC osteoblastic differentiation. VSMCs were grown in calcification media with DETA-NONOate for 14 days in the presence or absence of KT582 and ALP activity at OD 405 nm was measured ($n = 6 \pm$ SEM, $^*P < 0.01$). (*E*) An analogue of cGMP, 8-bromo-cGMP, inhibits VSMC calcification. VSMCs were grown calcification media with or without 8-bromo-cGMP for 14 days. Then, calcium concentration in the cells was measured as described in Methods section ($n = 3$–6 SEM, $^*P < 0.01$, $^{**}P < 0.05$). (*F*) 8-bromo-cGMP inhibits VSMC calcification. VSMCs were grown in calcification media with or without 8-bromo-cGMP for 14 day and ALP activity at OD 405 nm was measured ($n = 3$–$6 \pm$ SEM, $^*P < 0.01$).

expression as they mature before mineralization.[22] Therefore, decreasing of ALP activity in calcifying VSMC blocks differentiation of VSMCs into osteoblastic cells. Furthermore, ALP can promote calcification by hydrolysing pyrophosphate. Thus, inhibition of ALP activity by NO may suppress calcification by a number of mechanisms. These findin suggest that NO regulates vascular calcification through inh biting mineralization of VSMCs and differentiation of VSM into osteoblastic cells. On the other hand, the expression NOS was induced in calcifying VSMCs. Our hypothesis is th

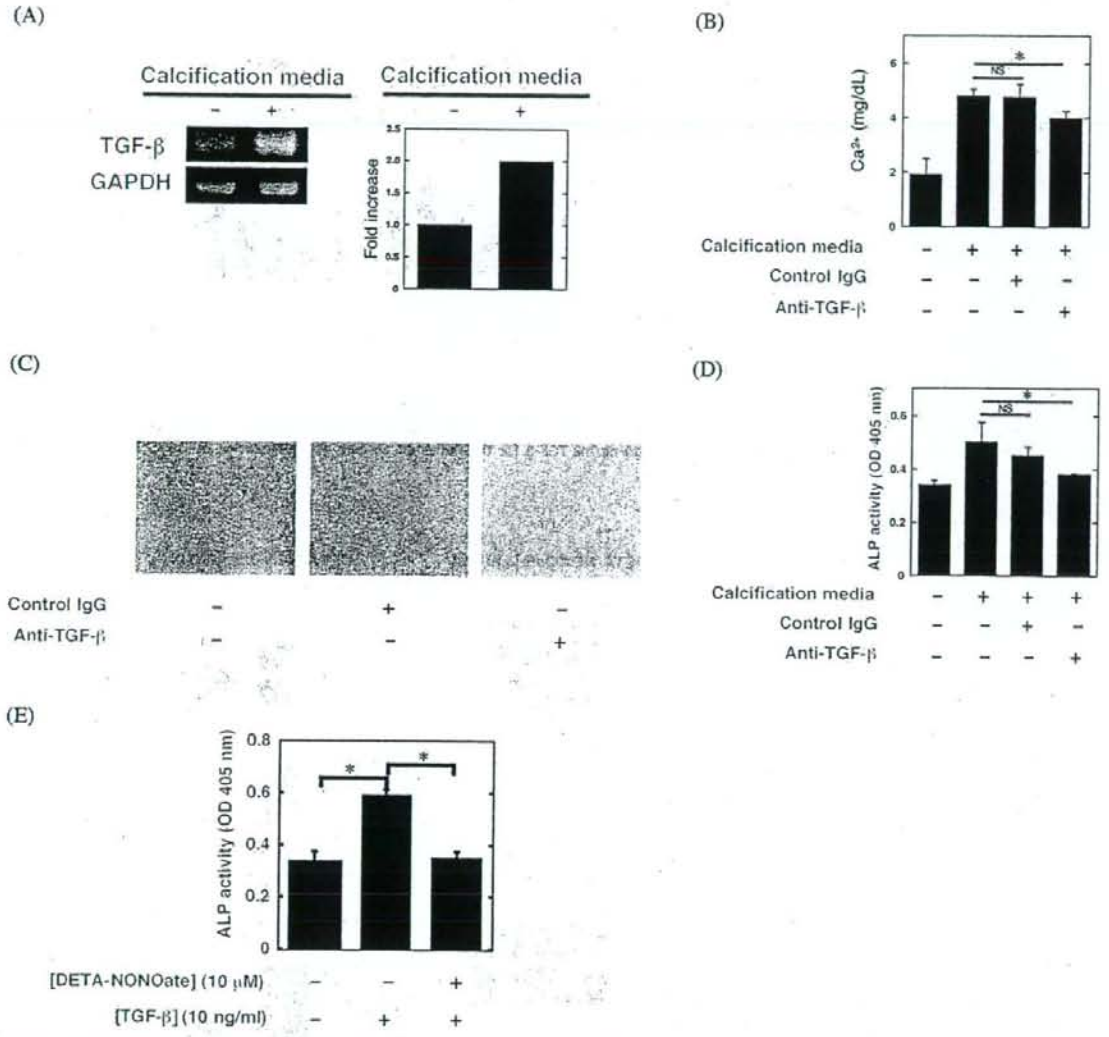

Figure 4 Transforming growth factor-β (TGF-β) induces vascular smooth muscle cell (VSMC) calcification. (*A*) TGF-β expression increases in calcifying VSMCs. VSMCs were grown for 14 days in the presence or absence of calcification medium. Then TGF-β gene expression in the cells was measured by RT-PCR. (*B*) Antibody to TGF-β inhibits VSMC calcification. VSMCs were grown in calcification media with various concentration of anti-TGF-β antibody or control IgG for 14 days. Then, calcium concentration in the cells was measured as described in Methods section ($n = 4$–$6 \pm$ SEM, $^*P < 0.05$). (*C*) Antibody to TGF-β inhibits VSMC calcification. VSMCs were grown in calcification media with various concentration of anti-TGF-β antibody or control IgG for 14 days. Then, cells were then stained with Alizarin red. (*D*) Antibody to TGF-β inhibits VSMC calcification. VSMCs were grown in calcification media with various concentration of anti-TGF-β antibody or control IgG for 14 days, and ALP activity at OD 405 nm was measured ($n = 4$–$6 \pm$ SEM, $^*P < 0.01$). (*E*) NO inhibits TGF-β induction of ALP activity. VSMCs were treated with DETA-NONOate for 2 days in the presence or absence of TGF-β. Then ALP activity in the cells was measured ($n = 5$–$6 \pm$ SEM, $^*P < 0.01$).

calcification medium induced NOS in VSMCs, where NOS is acting in a negative feedback loop. The degree of an increase in the expression of NOS isoforms was different respectively. NOS isoforms may play a different role in the negative feedback. In addition, other studies show that calcifying vascular cells, a subpopulation of cells from the artery wall and cardiac valves, have the ability to undergo osteoblastic differentiation and mineralization, and these cells have the potential for multiple lineages similar to mesenchymal stem cells.[25] Primary VSMCs might contain these cells. These cells may also have the ability to differentiate into the other type cells. Therefore, nNOS may be expressed in calcifying vascular cells though nNOS was absent in VSMCs. Further investigation would be required to clarify the details.

How does nitric oxide inhibit vascular calcification?

NO activates soluble guanylyl cyclase to produce cGMP that is involved in the relaxant response of VSMCs. Thus, we examined the effect of the guanylate cyclase inhibitor (ODQ) and PKG inhibitor (KT5823) on calcification and osteoblastic differentiation of VSMCs following NO treatment.

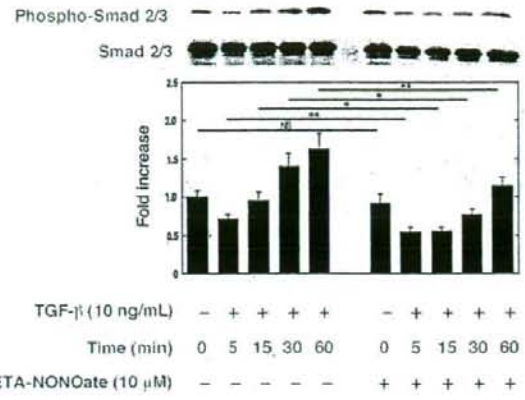

Figure 5 Nitric oxide (NO) regulates transforming growth factor-β (TGF-β) signalling in vascular smooth muscle cells (VSMCs). VSMCs were pretreated w DETA-NONOate for 60 min and then stimulated with 10 ng/mL TGF-β for the indicated periods. Phosphorylation of Smad2/3 was measured by western b

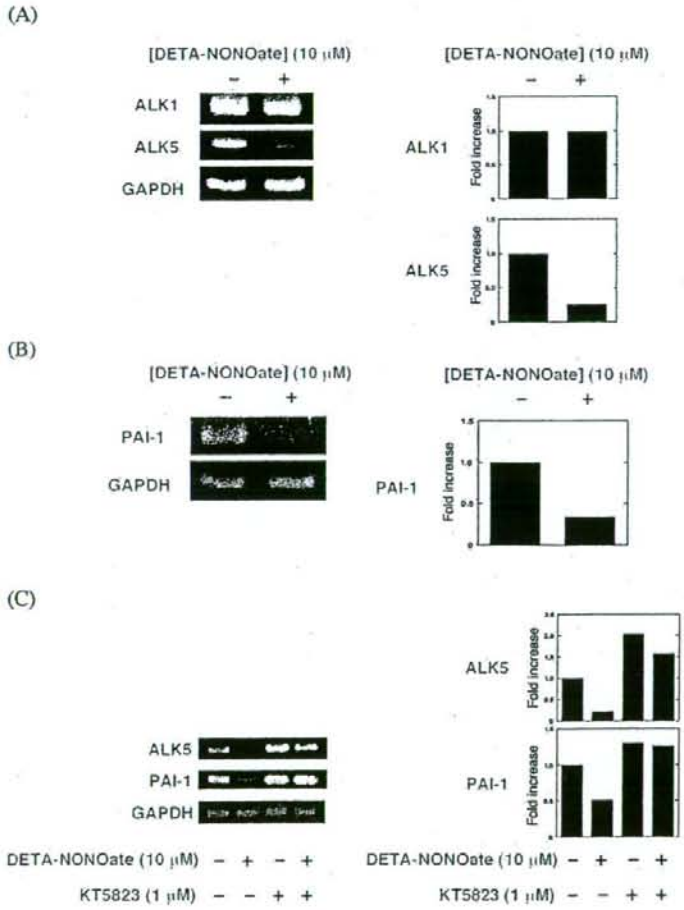

Figure 6 Nitric oxide (NO) inhibits transforming growth factor-β (TGF-β)-induced gene expression. (*A*) Effect of NO on ALK1 and ALK5 gene expression. Vascu smooth muscle cells (VSMCs) were grown in calcification media with 10 μM DETA-NONOate for 14 days. Then ALK1 and ALK5 gene expression in the cells w measured by RT-PCR. (*B*) Effect of NO on PAI-1 gene expression. Calcifying VSMCs were grown with 10 μM DETA-NONOate for 14 days. Then PAI-1 gene expressi in the cells was measured by RT-PCR. (*C*) KT5823 blocks NO inhibition of ALK5 and PAI-1 gene expression. VSMCs were grown in calcification media with DET NONOate for 14 days in the presence or absence of KT5823, then ALK5 and PAI-1 gene expression in the cells was measured by RT-PCR. Similar results we obtained with three additional and different samples.

Inhibition of guanylate cyclase and PKG reversed the inhibitory effect of NO on vascular calcification and osteoblastic differentiation of VSMCs. Treatment of calcifying VSMCs with cGMP analogue inhibited vascular calcification and osteoblastic differentiation. These results suggest that NO regulates vascular calcification in part through the action of cGMP. However, ODQ and KT5823 did not increase VSMC calcification in the absence of NO donor. On the other hand, ODQ and KT5823 increased osteoblastic differentiation in the absence of NO donor. These data show that another possibility remains that is additional cGMP independent pathways such as S-nitrosylation of proteins by NO may also regulate calcification. We speculate as follows. First, osteoblastic differentiation is increased in VSMCs. Second, calcium accumulates in osteoblastic VSMCs. Finally, VSMC calcification is increased. cGMP/PKG signalling pathway may inhibit osteoblastic differentiation and NO may inhibit both VSMC calcification and osteoblastic differentiation. Further investigations would be required to clarify the details.

TGF-β can act as an anti-inflammatory and anti-atherogenic cytokine with a protective role in the complications of atherosclerosis. However, TGF-β also regulates vascular smooth muscle differentiation and vascular calcification.[6,15] We showed that NO reduced TGF-β signalling by decreasing expression of a TGF-β receptor ALK5, resulting in a down-regulation of TGF-β signal that induces phosphorylation of Smad2/3. TGF-β transduce signals via two distinct type I receptors, ALK1 and ALK5.[26] ALK5 induces phosphorylation of Smad2/3, while ALK1 induces phosphorylation of Smad1/5. Our results suggest that TGF-β signal via ALK5/Smad2/3 in VSMC is important for inducing vascular calcification. In addition, KT5823 reversed the inhibitory effect of NO on the ALK5 gene expression. Recently, Saura *et al.*[27] have shown that NO regulates the transcriptional responses to TGF-β by inhibiting Smad nuclear accumulation via PKG activation in ECs. This important study suggests a molecular mechanism by which NO regulates TGF-β signalling in calcification. We also found that NO regulates the TGF-β/ ALK5/Smad2/3 signalling, inhibiting TGF-β-induced gene expression of PAI-1. In addition, KT5823 reversed the inhibitory effect of NO on the PAI-1 gene expression. The fibrinolytic system plays an important role in vascular and tissue housekeeping. PAI-1 plays a key role in regulating the fibrinolytic system by serving as the primary inhibitor of t-PA and u-PA. Several groups have reported excess PAI-1 in atherosclerotic plaques in humans,[28–30] a finding that is exaggerated in type 2 diabetics.[31] These studies suggest that PAI-1 plays an important role in atherosclerosis. PAI-1 may also play an important role in vascular calcification. Inhibition of PAI-1 gene expression by NO may have an important role of calcification in VSMCs. Further investigations would be required to clarify the details.

Clinical aspects of nitric oxide and vascular calcification

NO inhibits vascular inflammation: vascular injury and atherosclerosis are more severe in knockout mice lacking eNOS or iNOS; conversely, gene therapy with NOS ameliorates arteriosclerosis.[32–35] Patients with endothelial dysfunction and defective NO synthesis is at increased risk for cardiovascular events. Our data suggest that NO and compounds that induce NO synthesis may be useful not only in inhibiting vascular inflammation, but also in preventing vascular calcification.

Supplementary material

Supplementary material is available at *Cardiovascular Research* online.

Funding

This work was supported in part by grants from Mitsui, Life Social Welfare Foundation, Aichi Cancer Research Foundation, Mitsubishi Pharma Research Foundation, Mochida Memorial Foundation for Medical and Pharmaceutical Research, and Suzuken Memorial Foundation.

Conflict of interest: All authors have no conflict of interest.

References

1. Rumberger JA, Simons DB, Fitzpatrick LA, Sheedy PF, Schwartz RS. Coronary artery calcium area by electron-beam computed tomography and coronary atherosclerotic plaque area. A histopathologic correlative study. *Circulation* 1995;92:2157–2162.
2. Abedin M, Tintut Y, Demer LL. Vascular calcification: mechanisms and clinical ramifications. *Arterioscler Thromb Vasc Biol* 2004;24:1161–1170.
3. Hruska KA, Mathew S, Saab G. Bone morphogenetic proteins in vascular calcification. *Circ Res* 2005;97:105–114.
4. Ehara S, Kobayashi Y, Yoshiyama M, Shimada K, Shimada Y, Fukuda D *et al.* Spotty calcification typifies the culprit plaque in patients with acute myocardial infarction: an intravascular ultrasound study. *Circulation* 2004; 110:3424–3429.
5. Blacher J, Guerin AP, Pannier B, Marchais SJ, London GM. Arterial calcifications, arterial stiffness, and cardiovascular risk in end-stage renal disease. *Hypertension* 2001;38:938–942.
6. Watson KE, Bostrom K, Ravindranath R, Lam T, Norton B, Demer LL. TGF-beta 1 and 25-hydroxycholesterol stimulate osteoblast-like vascular cells to calcify. *J Clin Invest* 1994;93:2106–2113.
7. Otto CM, Kuusisto J, Reichenbach DD, Gown AM, O'Brien KD. Characterization of the early lesion of 'degenerative' valvular aortic stenosis. Histological and immunohistochemical studies. *Circulation* 1994;90: 844–853.
8. Sato Y, Nakamura R, Satoh M, Fujishita K, Mori S, Ishida S *et al.* Thyroid hormone targets matrix Gla protein gene associated with vascular smooth muscle calcification. *Circ Res* 2005;97:550–557.
9. Shanahan CM, Cary NR, Metcalfe JC, Weissberg PL. High expression of genes for calcification-regulating proteins in human atherosclerotic plaques. *J Clin Invest* 1994;93:2393–2402.
10. Trion A, Laarse van der A. Vascular smooth muscle cells and calcification in atherosclerosis. *Am Heart J* 2004;147:808–814.
11. Ross R. The pathogenesis of atherosclerosis–an update. *N Engl J Med* 1986;314:488–500.
12. Schwartz SM, Campbell GR, Campbell JH. Replication of smooth muscle cells in vascular disease. *Circ Res* 1986;58:427–444.
13. Dhore CR, Cleutjens JP, Lutgens E, Cleutjens KB, Geusens PP, Kitslaar PJ *et al.* Differential expression of bone matrix regulatory proteins in human atherosclerotic plaques. *Arterioscler Thromb Vasc Biol* 2001;21: 1998–2003.
14. Jian B, Narula N, Li QY, Mohler ER III, Levy RJ. Progression of aortic valve stenosis: TGF-beta1 is present in calcified aortic valve cusps and promotes aortic valve interstitial cell calcification via apoptosis. *Ann Thorac Surg* 2003;75:457–465.
15. Grainger DJ, Metcalfe J, Grace AA, Mosedale DE. Transforming growth factor-beta dynamically regulates vascular smooth muscle differentiation in vivo. *J Cell Sci* 1998;111:2977–2988.
16. Nathan C, Xie Q. Nitric oxide synthases: roles, tolls, and controls. *Cell* 1994;78:915–918.
17. Stamler JS, Singel DJ, Loscalzo J. Biochemistry of nitric oxide and its redox-activated forms. *Science* 1992;258:1898–1902.

18. Dubey RK, Jackson EK, Luscher TF. Nitric oxide inhibits angiotensin II-induced migration of rat aortic smooth muscle cell. Role of cyclic-nucleotides and angiotensin1 receptors. *J Clin Invest* 1995;**96**:141-149.
19. Garg UC, Hassid A. Nitric oxide-generating vasodilators and 8-bromo-cyclic guanosine monophosphate inhibit mitogenesis and proliferation of cultured rat vascular smooth muscle cells. *J Clin Invest* 1989;**83**:1774-1777.
20. Ross R, Glomset J, Kariya B, Harker L. A platelet-dependent serum factor that stimulates the proliferation of arterial smooth muscle cells in vitro. *Proc Natl Acad Sci USA* 1974;**71**:1207-1210.
21. Tintut Y, Parhami F, Bostrom K, Jackson SM, Demer LL. cAMP stimulates osteoblast-like differentiation of calcifying vascular cells. Potential signaling pathway for vascular calcification. *J Biol Chem* 1998;**273**:7547-7553.
22. Stein GS, Lian J, Stein JL, Van Wijnen AJ, Montecino M. Transcriptional control of osteoblast growth and differentiation. *Physiol Rev* 1996;**76**: 593-629.
23. Massague J. TGF-beta signal transduction. *Annu Rev Biochem* 1998;**67**: 753-791.
24. Wrana JL, Attisano L, Wieser R, Ventura F, Massagué J. Mechanism of activation of the TGFβ receptor. *Nature* 1994;**370**:341-347.
25. Tintut Y, Alfonso Z, Saini T, Radcliff K, Watson K, Boström K *et al*. Multilineage potential of cells from the artery wall. *Circulation* 2003;**108**: 2505-2510.
26. Goumans MJ, Valdimarsdottir G, Itoh S, Rosendahl A, Sideras P, ten Dijke P. Balancing the activation state of the endothelium via two distinct TGF-beta type I receptors. *EMBO J* 2002;**21**:1743-1753.
27. Saura M, Zaragoza C, Herranz B, Griera M, Diez-Marques L, Rodriguez-Puyol D *et al*. Nitric oxide regulates transforming growth factor-beta signaling in endothelial cells. *Circ Res* 2005;**97**:1115-1123.
28. Schneiderman J, Sawdey MS, Keeton MR, Bordin GM, Bernstein Dilley RB *et al*. Increased type 1 plasminogen activator inhibitor ge expression in atherosclerotic human arteries. *Proc Natl Acad Sci U* 1992;**89**:6998-7002.
29. Raghunath PN, Tomaszewski JE, Brady ST, Caron RJ, Okada Barnathan ES. Plasminogen activator system in human coronary athe sclerosis. *Arterioscler Thromb Vasc Biol* 1995;**15**:1432-1443.
30. Lupu F, Bergonzelli GE, Heim DA, Cousin E, Genton CY, Bachmann F *et* Localization and production of plasminogen activator inhibitor-1 human healthy and atherosclerotic arteries. *Arterioscler Thromb* 19 **13**:1090-1100.
31. Sobel BE, Woodcock-Mitchell J, Schneider DJ, Holt RE, Marutsuka Gold H. Increased plasminogen activator inhibitor type 1 in coron artery atherectomy specimens from type 2 diabetic compared with n diabetic patients. *Circulation* 1998;**97**:2213-2221.
32. Dusting GJ, Macdonald PS. Endogenous nitric oxide in cardiovasc disease and transplantation. *Ann Med* 1995;**27**:395-406.
33. Qian Z, Gelzer-Bell R, Yang Sx SX, Cao W, Ohnishi T, Wasowska BA *al*. Inducible nitric oxide synthase inhibition of weibel-palade b release in cardiac transplant rejection. *Circulation* 2001;1 2369-2375.
34. Knowles JW, Reddick R, Jennette JC, Shesely EG, Smithies O, Maeda Enhanced atherosclerosis and kidney dysfunction in eNOS(−/− Apoe(−/−) mice are ameliorated by enalapril treatment. *J Clin In* 2000;**105**:451-458.
35. West NE, Qian H, Guzik TJ, Black E, Cai S, George SE *et al*. Nitric ox synthase (nNOS) gene transfer modifies venous bypass graft remodel effects on vascular smooth muscle cell differentiation and superox production. *Circulation* 2001;**104**:1526-1532.

ELSEVIER

INSTITUT PASTEUR

Microbes and Infection 9 (2007) 1500–1506

www.elsevier.com/locate/micinf

Original article

Arginine-specific gingipain A from *Porphyromonas gingivalis* induces Weibel-Palade body exocytosis and enhanced activation of vascular endothelial cells through protease-activated receptors

Megumi Inomata [a,b], Takeshi Into [a,*], Yuichi Ishihara [b], Misako Nakashima [a], Toshihide Noguchi [b], Kenji Matsushita [a]

[a] *Department of Oral Disease Research, National Institute for Longevity Sciences, National Center for Geriatrics and Gerontology, 36-3 Gengo, Morioka, Obu, Aichi 474-8522, Japan*

[b] *Department of Periodontology, School of Dentistry, Aichigakuin University, Nagoya, Japan*

Received 15 May 2007; accepted 9 August 2007
Available online 23 August 2007

Abstract

Gingipains, cysteine proteases derived from *Porphyromonas gingivalis*, are important virulence factors in periodontal diseases. We found that arginine-specific gingipain A (RgpA) increased the responsiveness of vascular endothelial cells to *P. gingivalis* lipopolysaccharides (LPS) and *P. gingivalis* whole cells to induce enhanced IL-8 production through protease-activated receptors (PARs) and phospholipase C (PLC) γ. We therefore investigated whether RgpA-induced enhanced cell activation is mediated through exocytosis of Weibel-Palade bodies (WPBs) because they store vasoactive substances. RgpA rapidly activated PAR- and PLCγ-dependent WPB exocytosis. In addition, angiopoietin (Ang)-2, a substance of WPB, enhanced IL-8 production by *P. gingivalis* LPS, suggesting that Ang-2 mediates the RgpA-induced enhanced cell responses. Thus, we propose a novel role for RgpA in induction of a proinflammatory event through PAR-mediated WPB exocytosis, which may be an important step for enhanced endothelial responses to *P. gingivalis*.

Keywords: Gingipain; *Porphyromonas gingivalis*; Vascular endothelial cells; Weibel-Palade body; Exocytosis; Protease-activated receptors; Periodontitis

1. Introduction

Porphyromonas gingivalis is a principal periodontopathic pathogen [1,2]. Although *P. gingivalis* has a number of virulence factors, including lipopolysaccharide (LPS) and fimbriae, the most notable factors are the cysteine proteases termed gingipains. Two kinds of arginine residue-specific gingipains, RgpA and RgpB, and another type of lysine residue-specific gingipain have so far been identified [3–5]. Gingipains associated with released vesicles from *P. gingivalis* cells especially exert various pathophysiological effects through cleavage or degradation of in-host proteins, such as tissue proteins, coagulation factors and cytokines.

Microvessels are thought to be one of the first lines of defense against *P. gingivalis* in periodontal tissue. *P. gingivalis* promotes transmigration of neutrophils and monocytes from blood vessels into periodontal tissue and increase vascular permeability. Proinflammatory effects of *P. gingivalis* are thought to be dependent on gingipain-induced activation of vascular endothelial cells to induce an increase in vascular permeability, cytokine production and adhesion molecule expression [6,7].

Abbreviations: Ang, angiopoietin; GAPDH, glyceraldehydes-3-phosphate dehydrogenase; HKPG, heat-killed whole cells of *P. gingivalis*; HUVEC, human umbilical vein endothelial cell; LPS, lipopolysaccharide; PLC, phospholipase C; PAR, protease-activated receptor; RgpA, arginine-specific gingipain A; siRNA, short interfering RNA; TLR, Toll-like receptor; VWF, von Willebrand factor; WPB, Weibel-Palade body.

* Corresponding author. Tel.: +81 562 44 5651x5064; fax: +81 562 46 8684.
E-mail address: into@nils.go.jp (T. Into).

1286-4579/$ - see front matter © 2007 Elsevier Masson SAS. All rights reserved.
doi:10.1016/j.micinf.2007.08.005

In this study, we explored gingipain-induced responses of vascular endothelial cells in detail. We found that RgpA induces degranulation and modulates *P. gingivalis*-induced proinflammatory responses of endothelial cells through the release of storage substances, in which protease-activated receptor (PAR)-mediated signaling plays an important role.

2. Materials and methods

2.1. Reagents, chemicals and cell culture

A23187, U73122, 1,2-bis (2-aminophenoxy) ethane-*N*,*N*,*N*′,*N*′-tetraacetic acid–acetoxymethyl ester (BAPTA–AM) and highly purified LPS from *Escherichia coli* were purchased from Sigma–Aldrich (St Louis, MO). Leupeptin was purchased from Peptide Institute (Osaka, Japan). Preparation of vesicle-associated RgpA from *P. gingivalis* HG66 in culture media was described previously [8]. Purified LPS from *P. gingivalis* ATCC33277, heat-killed whole cells of *P. gingivalis* (HKPG) ATCC33277 and the synthetic bacterial lipopeptide Pam_3CSK_4 were obtained from InvivoGen (San Diego, CA). Recombinant human interleukin (IL)-1β and angiopoietin-2 (Ang-2) were obtained from R&D systems (Minneapolis, MN). Human umbilical vein endothelial cells (HUVECs) were grown as described previously [9]. Cells were used for experiments from passages 4 to 8.

2.2. RNA interference in HUVECs

Gene-specific short interfering RNAs (siRNAs) for human PARs, human Ang-2 and a control oligonucleotide were purchased from Dharmacon (Chicago, IL). RNA interference in HUVEC was performed according to the method described previously [9].

2.3. Determination of von Willebrand factor (VWF) by ELISA

Confluent HUVECs seeded on 24-well plates were prepared in serum-free EGM-2 media. Cells were stimulated for 1 h with RgpA. The culture media were collected and clarified for analyses of the amounts of VWF as described previously [9].

2.4. Determination of interleukin IL-8 by ELISA

Confluent HUVECs seeded on 24-well plates were stimulated for 6 h with *P. gingivalis* LPS or HKPG in the presence or absence of 200 nM RgpA. Then the culture media were collected and clarified for analyses of the amounts of IL-8 using a human IL-8 ELISA kit (Invitrogen) according to the manufacturer's instructions. Results are representative of three separate experiments and are expressed as means ± standard deviation (SD) of triplicate wells.

2.5. Quantitative RT-PCR

Total RNA was extracted using an RNeasy Mini ki
GEN, Valencia, CA). Transcripts were quantified by re
quantitative PCR on a LightCycler ST300 system (Roc
values were normalized to the level of glyceraldehydes-
phate dehydrogenase (GAPDH) mRNA. The primer sets
follows: human PAR_1: sense, 5′-cccgctgttgtctgccc-3′ a
sense, 5′-ggttcctgagaagaaatgaccg-3′; human PAR_2: se
gaggtattgggtcatcg-3′ and antisense, 5′-ggctgggaacag
human PAR_3: sense, 5′-ggacaggagccacgat-3′ and an
5′-ccacagggtcacagca-3′; human PAR_4: sense, 5′-agc
caatcct-3′ and antisense, 5′-cagccatgcagagtccaa-3′;
GAPDH: sense, 5′-gaaggtgaaggtcggagtc-3′ and an
5′-gaagatggtgatgggatttc-3′; human Ang-1: sense, 5′
aaccgagcc-3′ and antisense, 5′-gggcacatttgcaca-3′; hun
-2: sense, 5′-ccacaaatggcatctacacg-3′ and a
5′-cccagccaatattctcctga-3′; and human IL-8: sense, 5′-
ccttcctgatttc-3′ and antisense, 5′-tcagccctcttcaaaaacttc
PCR amplicons were visualized on 1.5% agarose gels
with ethidium bromide and photographed under U
Results are representative of three separate experiment

2.6. Immunofluorescence of Ang-2 and VWF

Confluent HUVECs were prepared and fixed at
with methanol for 60 min. Immunostaining was carrie
ing an anti-Ang-2 rabbit polyclonal antibody (Santa C
technology) and Alexa Fluor 488-conjugated anti-ra
antibody (Invitrogen). Images were obtained by a flu
microscope IX71 (magnification ×40) with DP7
capture (Olympus).

2.7. Statistical analysis

All values were evaluated by statistical analyses u
dent's *t*-test. Differences were considered to be sta
significant at the level of $P < 0.01$.

3. Results

3.1. Effect of RgpA on the early-phase inflammatory response in HUVECs

We first investigated the effect of RgpA on *P. g*
induced inflammatory responses of vascular endothe
HUVECs responded to RgpA, *P. gingivalis* LPS and
induce IL-8 production (Fig. 1A). RgpA synergically
gistically enhanced IL-8 production by *P. gingivalis*
HKPG (Fig. 1A). We also found that RgpA could u
IL-8 production by *E. coli* LPS, Pam_3CSK_4 an
(Fig. 1B). It has been reported that RgpA directl
proinflammatory responses through PAR activati
PARs are a family of G protein-coupled receptors th
cleavage at the N-terminus to be activated [11,12]
four members of PARs, HUVECs expressed mI
PAR_1, PAR_2 and PAR_3 but not that of PAR_4 (Fig.

data not shown). We utilized siRNAs to investigate the role of PARs, which could effectively reduce each PAR mRNA expression (Fig. 1C). We confirmed that transfection of the mixture of siRNAs for PAR_{1-3} could simultaneously reduce the expression of PAR_{1-3} (Fig. 1C). The upregulatory effect of RgpA on IL-8 production was reduced by knockdown of PAR_{1-3} (Fig. 1D). We also found that inhibition of PLCγ, a common mediator of PAR signaling, by U73122 abolished RgpA-induced enhanced IL-8 production (Fig. 1E). Thus, the PAR–PLCγ pathway plays a crucial role in RgpA-induced enhanced activation of vascular endothelial cells.

3.2. RgpA activates Weibel-Palade body exocytosis

Because early endothelial activation involves degranulation of the endothelial cell-specific granules Weibel-Palade bodies

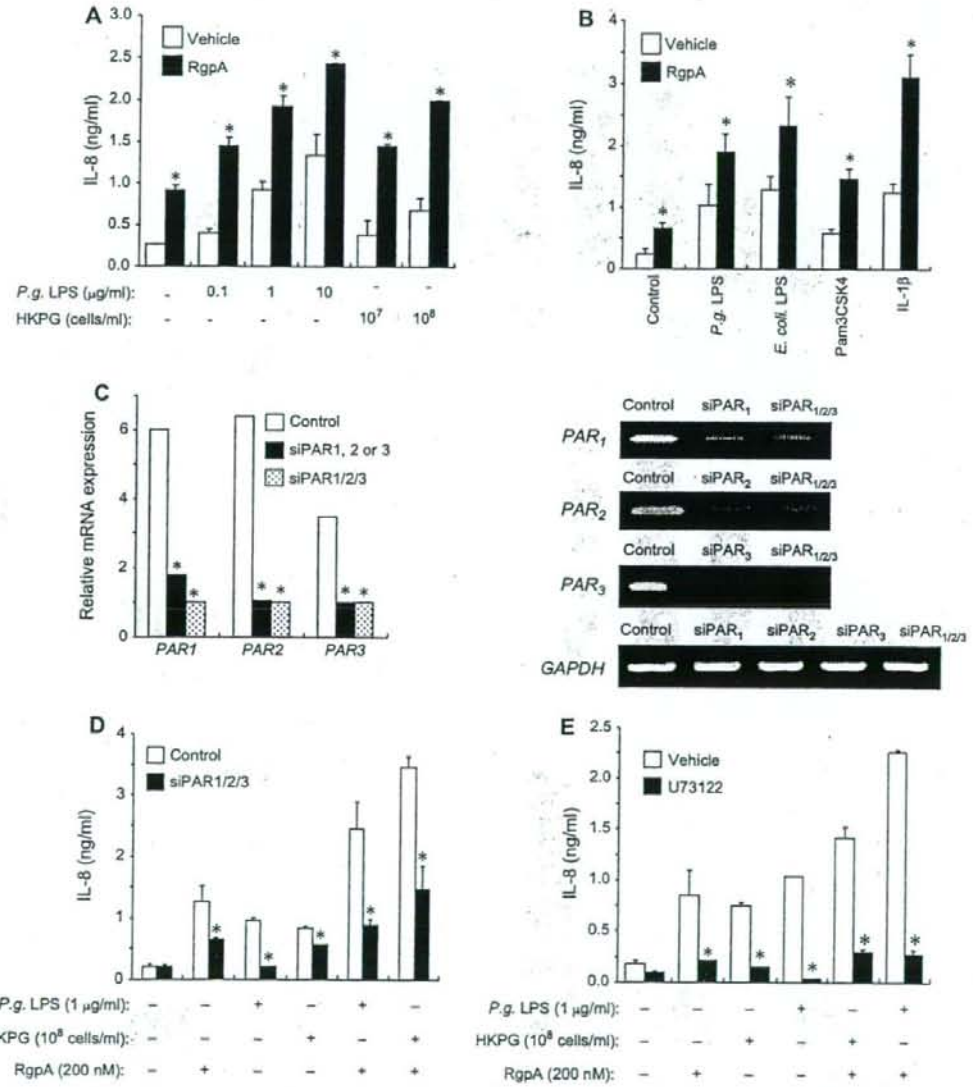

Fig. 1. Effect of RgpA on IL-8 production induced by *P. gingivalis* LPS or HKPG. (A, B) HUVECs were stimulated for 6 h with the indicated concentrations of LPS or HKPG (A) or with *E. coli* LPS (10 ng/ml), *P. gingivalis* LPS (1 μg/ml), Pam_3CSK_4 (0.5 μg/ml) or IL-1β (1 ng/ml) (B) in the presence or absence of 200 nM RgpA. The amounts of IL-8 released into the media were measured by ELISA. Each value is the mean ± SD ($n = 3$) *vs control group, $P < 0.01$. (C) HUVECs were transfected with siRNA for PAR_1, PAR_2 or PAR_3 or together with these siRNAs. The expression levels of mRNAs of PAR_1, PAR_2 and PAR_3 were determined by quantitative RT-PCR *vs control group, $P < 0.01$. (D, E) HUVECs were transfected together with siRNAs for PAR_1, PAR_2 and PAR_3 (D) or pretreated for 30 min with 10 μM U73122 (E). Cells were then stimulated for 6 h with 1 μg/ml *P. gingivalis* LPS or 10^8 cells/ml HKPG in the presence or absence of 200 nM RgpA. The amounts of IL-8 released into the media were measured by ELISA. Each value is the mean ± SD ($n = 3$) *vs control group, $P < 0.01$.

(WPBs) [13–15], we thought to determine whether RgpA-induced activation of vascular endothelial cells is affected by WPB exocytosis. We first examined whether RgpA could activate Weibel-Palade body exocytosis in HUVEC. Quantification of exocytosis was performed by measuring the amount of VWF, an essential constituent of WPBs. RgpA-induced VWF release in a similar manner to the calcium ionophore A23187 (Fig. 2A). The release of VWF occurred within 5 min and continued for at least 60 min after stimulation (Fig. 2B ence of the cysteine protease inhibitor leupeptin reduced induction of VWF release by RgpA but not A23187 (Fig. 2C), suggesting that RgpA-induced exo depends on its protease activity.

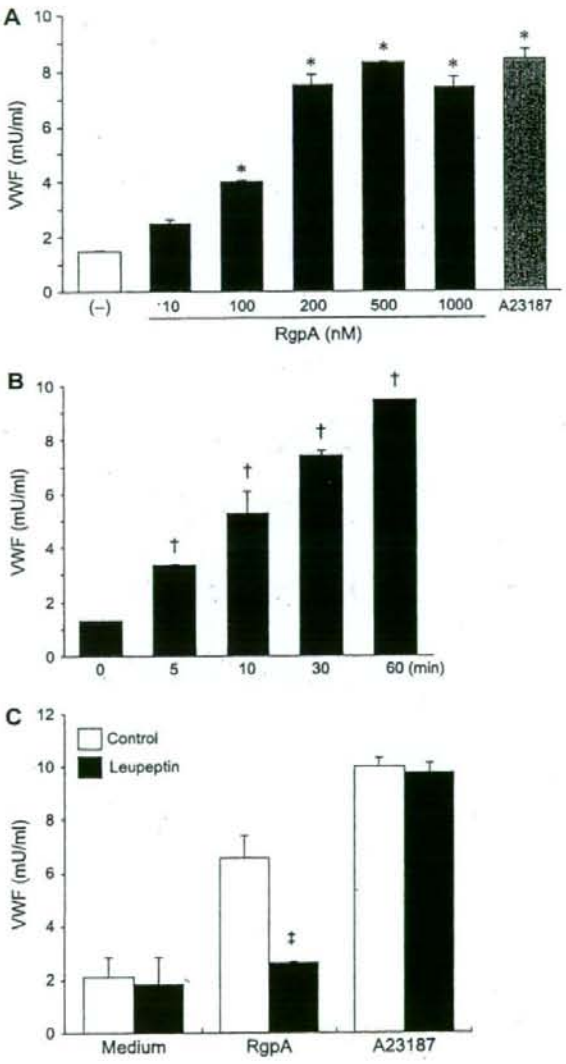

Fig. 2. Induction of WPB exocytosis by RgpA. (A) HUVECs were stimulated for 1 h with RgpA at the indicated concentrations or with 10 μM A23187. (B) HUVECs were stimulated with 200 nM RgpA for the indicated periods. (C) HUVECs were stimulated for 1 h with 200 nM RgpA or 10 μM A23187 in the presence or absence of 2 μM leupeptin. The amounts of VWF released into the media were measured by ELISA. Each value is the mean ± SD ($n = 3$) *vs vehicle group, $P < 0.01$; †vs '0 min', $P < 0.01$; and ‡vs control group, $P < 0.01$.

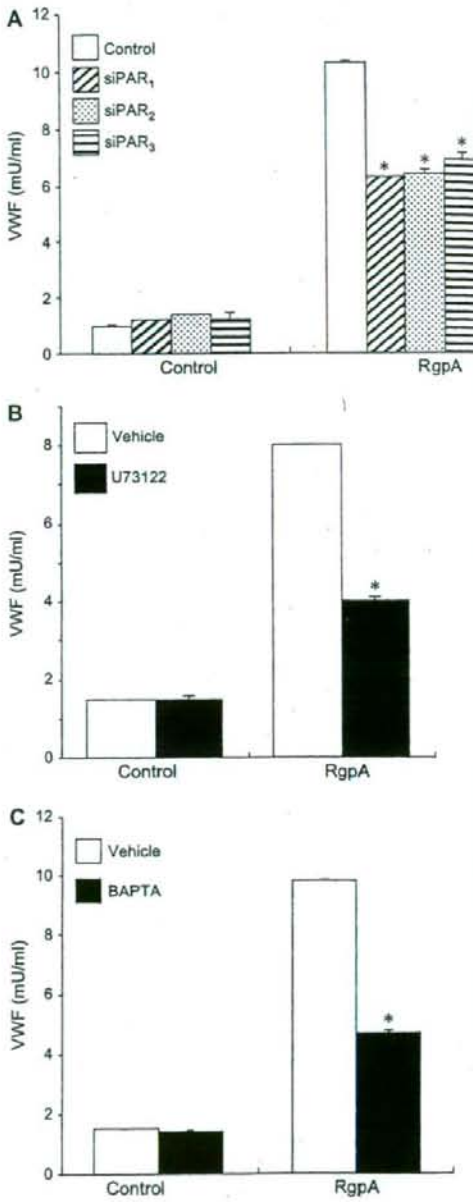

Fig. 3. Regulatory mechanisms of RgpA-activated WPB exocytosis VECs transfected with siRNAs for PAR_1, PAR_2 or PAR_3 were stim 1 h with 200 nM RgpA or 10 μM A23187. (B) HUVECs pretreated with 10 μM U73122 were stimulated for 1 h with 200 nM RgpA. (C) pretreated for 30 min with 20 μM BAPTA–AM were stimulated fo 200 nM RgpA. The amounts of VWF released into the media were by ELISA. Each value is the mean ± SD ($n = 3$) *vs control group,

3.3. RgpA activates WPB exocytosis through the PAR–PLCγ pathway

We next examined whether RgpA-induced WPB exocytosis was mediated by PARs and PLCγ. As shown in Fig. 3A, transfection of respective PAR siRNA could significantly suppress RgpA-induced VWF release. Common regulated WPB exocytosis is activated through an increase in intracellular Ca^{2+} level after stimulation with various secretagogues [13,14]. In addition, PLCγ is known as a regulator of intracellular calcium release by the generation of inositol (1,4,5) triphosphate. We found that the PLCγ inhibitor U73122 decreased RgpA-induced VWF release (Fig. 3B). Furthermore, RgpA-induced VWF release was significantly suppressed by the cell-permeable Ca^{2+} chelator BAPTA–AM (Fig. 3C). Thus, RgpA activates intracellular Ca^{2+}-dependent WPB exocytosis through the PAR–PLCγ pathway.

3.4. Effect of WPB components on P. gingivalis-induced inflammatory responses

We finally investigated whether released substances from WPB affect the RgpA-induced enhanced cell activation. Among known substances of WPB, we focused on the Tie-2 receptor ligand and Ang-2 because Ang-2 is known to enhance TNF-α-induced proinflammatory responses in HUVECs [16]. HUVECs expressed mRNA of Ang-2, but not that of another Tie-2 ligand Ang-1 (Fig. 4A). Stimulation with *P. gingivalis* LPS did not alter these expressions (Fig. 4A). Ang-2 protein was localized in granules (Fig. 4B). We found that recombinant Ang-2 added to the culture increased IL-8 production by *P. gingivalis* LPS (Fig. 4C). Furthermore, knockdown of Ang-2 suppressed IL-8 expression induced by *P. gingivalis* LPS (Fig. 4D). Thus, Ang-2 has a role to mediate the enhanced activation of endothelial cells.

4. Discussion

PARs play important roles in the regulation of several physiological and pathological effects, including coagulation, inflammation and vascular homeostasis [11,12,17]. We found that endothelial PARs were involved in RgpA induction of WPB exocytosis and regulation of endothelial cell activation. PAR-mediated responses in endothelial cells are known to be activated by thrombin. Thrombin stimulation elicits a capillary leak in vivo and increased endothelial monolayer permeability in vitro [18,19]. In addition, thrombin activates WPB exocytosis via PAR_1 or PAR_2 [20]. Thus, in a way similar to thrombin,

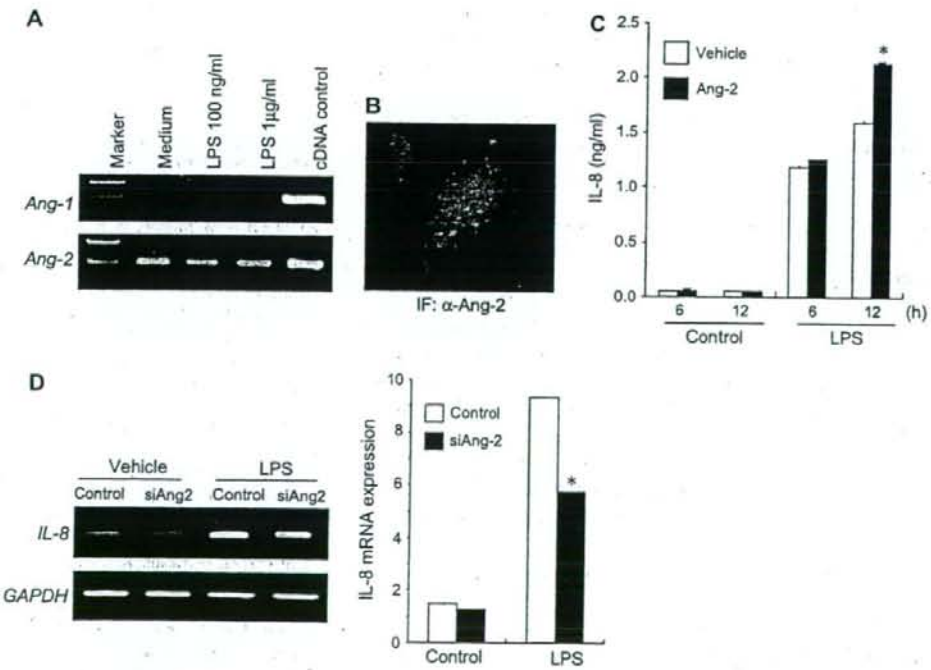

Fig. 4. Effect of Ang-2 on IL-8 production by *P. gingivalis* LPS. (A) Total RNA of HUVECs stimulated for 6 h with or without given concentrations of LPS was extracted for RT-PCR using specific primer sets for Ang-1 or Ang-2. The cDNA of Ang-1 and Ang-2 were used as templates for positive controls. (B) HUVECs were stained immunofluorescently with anti-Ang-2 antibody. Cell nuclei were stained with Höechst33342. (C) HUVECs were stimulated for 6 h or 12 h with 1 μg/ml *P. gingivalis* LPS in the presence or absence of 200 ng/ml recombinant Ang-2. The amounts of IL-8 released into the media were measured by ELISA. Each value is the mean ± SD ($n = 3$) *vs control group, $P < 0.01$. (D) HUVECs transfected with siRNA for Ang-2 were stimulated for 6 h with 1 μg/ml *P. gingivalis* LPS. The expression level of IL-8 mRNA was determined by quantitative RT-PCR *vs control group, $P < 0.01$.